ORIGINAL ARTICLE

A C G publications

Rec. Nat. Prod. 15:6 (2021) 487-502

records of natural products

Secondary Metabolites from *Teucrium creticum* L.

Azmi Hanoğlu [1], Duygu Yiğit Hanoğlu [2], Nilay Demirel [1], Hasan Soliman Yusufoğlu [3] and İhsan Çalış [1*]

[1]*Near East University, Faculty of Pharmacy, Department of Pharmacognosy, Lefkoşa, Turkish Republic of Northern Cyprus*
[2]*Near East University, Faculty of Pharmacy, Department of Pharmaceutical Botany, Lefkoşa, Turkish Republic of Northern Cyprus*
[3]*Prince Sattam Bin Abdulaziz University, Department of Pharmacognosy, Al-Kharj–11942, Saudi Arabia*

(Received December 29, 2020; Revised February 25, 2021; Accepted March 01, 2021)

Abstract: From the aerial parts of *Teucrium creticum* L. (Lamiaceae) eight compounds, **1 – 8** were isolated using chromatographical methods. Based on the results of spectroscopical analysis such as UV, 1D-NMR (^{1}H-, ^{13}C-NMR, DEPT-135), 2D-NMR (COSY, HSQC, HMBC, NOESY) and HRMS, the structure of the compounds were determined as two iridoids, 8-*O*-acetylharpagide (**1**) and teuhircoside (**2**), two phenylethanoid glycosides, verbascoside (= acteoside) (**3**) and lavandulifolioside (**4**), and four neoclerodane-type diterpenoids, teucrin H3 (= 19-acetylgnaphalin) (**5**), teucjaponin B (**6**), teucretol (**7**) and diacetylteumassilin (**8**).

Keywords: Lamiaceae; *Teucrium creticum;* iridoids; phenylethanoid glycosides; neo-clerodane-type diterpenoids.© 2021 ACG Publications. All rights reserved.

1. Introduction

Lamiaceae, the sixth largest Angiosperm family, contains more than 245 genera and 7886 species, and it is distributed worldwide for numerous species economically and medicinally valued [1]. In the last two decades, an improvement has been presented for its subfamilial classification [2]. According to the recent reports, Ajugoideae, Lamioideae, Nepetoideae, Prostantheroideae, Scutellarioideae, Symphorematoideae, Viticoideae, Cymarioideae, Peronematoideae, Premnoideae, Callicarpoideae and Tectonoideae have been recognized as subfamilies of Lamiaceae. Throughout the world, in the family Lamiaceae, *Teucrium* L. is one of the largest genera with 250 species. In the flora of Turkey, five subfamilies of Lamiaceae are to be found: Ajugoideae, Lamioideae, Nepetoideae, Scutellarioideae and Viticoideae. As a member of Ajugoideae, *Teucrium* genus is represented by 49 taxa in the flora of Turkey [1].

In the flora of Cyprus, *Teucrium* is represented by 9 species which are classified under the five sections, Teucrium (1 spec.), Polium (5 spec.), Chamaedrys (1 spec.), Scorodonia (1 spec.) and Scordium (1 spec., 2 ssps.) [3]. Present study has been performed on the *Teucrium creticum* L. which is a member of Teucrium section.

Extensive studies have been carried out on the phytochemical and pharmacological activities of the *Teucrium* species. In the legendary history of Cyprus, it is narrated that the medicinal properties

* Corresponding author: E-Mail: ihsan.calis@neu.edu.tr; Phone:+90 392-223 6464/5122

The article was published by ACG Publications
http://www.acgpubs.org/journal/records-of-natural-products October-December 2021 EISSN:1307-6167
DOI: http://doi.org/10.25135/rnp.232.20.12.1922

of *Teucrium* species was put in use for the first time by the founder and king of the city of Salamis in Cyprus - whose name Teucer is hence associated with the naming of the species as *Teucer, Teucru Teucros or Teucris* [4]. It is known that the representatives of the genus *Teucrium* have been used for more than 2000 years as medicinal herbs. The ethnopharmacological claims for *Teucrium* species include the use of decoctions, or infusions as stimulants, tonics, diaphoretics, diuretics; and, for treatments of stomach pain, asthma, amenorrhea, leucorrhoea, chronic bronchitis; and, for gout in traditional medicine. They have also been used as antispasmolytic, hypoglycemic agents and for CNS depressant activities [5]. *Teucrium polium* is documented to be used for the curing of pathophysiological maladies such as diabetes, gastrointestinal disorders, rheumatism, inflammations. Besides, the same species is also discovered to be useful in diuretic, antipyretic, tonic, diaphoretic, analgesic and antihyperlipidemic activities [6-8].

The *Teucrium* species contain number of compound classes, which especially include phenylethanoid (=phenylpropanoid) glycosides, iridoid glycosides and neo-clerodane diterpenoids. In 1985, poluimoside - a phenylpropanoid (=phenylethanoid) glycoside - was isolated from *Teucrium belion* by Andary and friends [9]. In 1988, Gross and friends reported teucrioside - another phenylpropanoid glycoside – isolated from *Teucrium chamaedrys* [10]. Teucrioside is the first L-lyxose containing phenylpropanoid glycoside found in nature. Also, in 1988, Andary and friends further made a chemotaxonomic study on the species, this time of *T. polium* examining the caffeic acid esters. Furthermore, several studies have demonstrated the wide range of biological and pharmacological activities of phenylethanoid glycosides, which are the main phenolic components, in *Teucrium* species [11].

The genus *Teucrium* is also one of the richest sources of clerodane-*type* diterpenoids [5]. Flavonoids and aromatic compounds, although furan containing neo-clerodane diterpenoids, have also been found in the genus [12]. Diterpenoids isolated from the aerial parts of *Teucrium* are those with a neoclerodane skeleton. More than 220 diterpenes have been described, all differing in the functional groups on the neoclerodane, or (on) the 19-nor-neoclerodane skeleton [13]. Neo-clerodane diterpenoids are accepted to be chemotaxonomic markers of the *Teucrium* species, which are known to be the most abundant natural source for these compounds. Teucrin A and teuchamaedryn A, classified as neo-clerodane diterpenoids, are natural toxic compounds. Their hepatoxicity is publicly confirmed after a 1992 dated incident, when out of 27 hepatoxicity cases in total – one resulting in death - the French Health Department forbid the sales of medicinal preparations containing *Teucrium chamaedrys*.

Since 1996, the Italian Ministry of Health considers its flowering tops used in teas as poison, as well as all the preparations obtained from *T. chamaedrys* [12]. The species of the genus *Teucrium* are very rich in phenolic compounds with very strong biological activity [14].

The aim of this study is to search secondary metabolites of *Teucrium creticum* L. *T. creticum* (Lat. “of Crete”) is found in Eastern Mediterranean region from Turkey to Palestine [3]. This study resulted in the isolation and structure elucidation of two iridoids that are 8-*O*-acetylharpagide (**1**) and teuhircoside (**2**); two phenylethanoid glycosides, verbascoside (= acteoside) (**3**) and lavandulifolioside (**4**), and four neoclerodane-type diterpenoids; teucrin H3 (= 19-acetylgnaphalin) (**5**), teucjaponin B (**6**), teucretol (**7**) and diacetylteumassilin (**8**) (Figure 1).

2. Materials and Methods

2.1. Plant Material

Teucrium creticum L. was collected from south hillside of St. Hilarion, Cyprus in 25 May 2018 and identified by Prof. Dr. İhsan ÇALIŞ (Department of Pharmacognosy, Faculty of Pharmacy, Near East University, Nicosia, Cyprus), Azmi Hanoğlu, Duygu Yiğit Hanoğlu. A voucher specimen (NEUN 1675) has been deposited in the NEUN Herbarium of the Near East University.

2.2. General Experimental Procedures

Classical column chromatography and a gradient Medium Pressure Liquid Chromatography (Büchi MPLC equipped by Pump Modules C-601 & C-605 with a pump Controller C-610 and pump

manager C-605) and a Büchi Fraction Collector C-615 were used for the isolation process. Silica gel (0.063–200 mμ, Merck), LiChroprep C-18 (0.063–200 mm, Merck) and Sephadex LH-20 were used as stationary phases throughout chromatographical studies. Silica gel alumina plates (Silica Gel 60 F_{254}, Merck) were used for Thin Layer Chromatography. Melting points were determined using an Electrothermal IA9200 Digital Programmable Melting Point Apparatus (Cole Parmer). Optical rotations were measured on a Schmidt+Haensch Polartronic MHZ-8 polarimeter. UV Spectra were recorded on a T70 UV-VIS Spectrometer (PG Instruments Ltd.). For 1D and 2H NMR experiments were performed using Varian and Brucker DRX 500 spectrometers (^{1}H-NMR; 400 and 500 MHz; ^{13}C-NMR: 100 and 150 MHz, resp.) using the XWIN NMR software package for the data acquisition and processing. Negative- and positive-mode HRMS were recorded on a Finnigan TSQ 7000 and HR-Mass Spectrometer and a UPLC-Quadrupole Orbitrap instrument. For lyophlization a CHRIST Alpha 1-4 LD Plus was used. Throughout the study, Büchi R-210 and Heidolph 4001 rotary evaporators were used.

2.3. Extraction

The air-dried and powdered aerial parts of the plant material (100 g) was extracted by maceration procedure using 80% ethyl alcohol (1000 mL) for 48 hours. After maceration, the extract was filtered with vacuum by using Buchner funnel. Solvent was removed from the extract by rotary evaporator under reduced pressure at 50 °C. During the concentration procedure, precipitated lipophilic compounds (chlorophil etc.) were removed by filtration. Water soluble part of the concentrated extract was fractionated by VLC.

2.3.1 Fractionation and Isolation Studies

Concentrated extract in water (50 mL) was subjected to a RP-VLC (50g LiChroprep RP-18) then fractionated by gradient elution using H_2O-MeOH mixtures with increasing amount of MeOH in H_2O (Water: Methanol 100:0 → 0:100). According to the TLC profile of the fractions, they were combined into six fractions; frs. 2 and 3 (Fr. A, 5.7 g), fr. 4 (Fr. B, 323 mg), mixture of frs. 5, 6 and 7 (Fr. C, 975 mg), mixture of frs. 8 and 9 (Fr. D, 2.218 g), fr. 10 (Fr. E, 1.391 g) and fr. 11 (Fr. F, 153 mg).

*2.3.1.1. Isolation of iridoids, **1** and **2***

4.8 g of fraction A (5.7 g) rich in sugars was coarsely fractionated over a short silica gel column (50 g) using eluent systems firstly DCM (100 mL) and a mixture of DCM-MeOH (9:1, 100 mL; 8:2, 100 mL; 7:3, 200 mL) and finally with DCM-MeOH-H_2O with an increasing polarity (80:20:2, 70:30:3 and 60:40:4; each 100 mL) (fraction volume: 50 mL). Fractions 7 – 12 (750 mg) were rich in **1** and **2** which was further applied to RP-MPLC (Stationary phase: LiChroprep C-18; Column dimensions: 25 mm × 250 mm; Fraction volume: 15 mL) using first H_2O (100 mL) and H_2O-MeOH mixture (gradient elution: 1 – 30% MeOH in H_2O; 1200 mL) and finally MeOH (200 mL) as eluents. Fractions 37 – 52 yielded **2** (150 mg), while fractions 70 – 86 yielded **1** (136 mg). Fraction B (323 mg) was also rich in **1** which was further applied to a silica gel column (30 g) using a solvent system DCM-MeOH-H_2O with an increasing polarity (90:10:1, 200 mL; 85.15.1, 100 mL; 80:20:2, 100 mL and 70:30:3, 100 mL) to yield **1** (132 mg).

*2.3.1.2. Isolation of phenylethanoid glycosides, **3** and **4***

2.13 g of fraction 8-9 (D) was subjected to a silica gel chromatography (130 g) with DCM-MeOH-H_2O mixtures with an increasing polarity (80:20:1→60:40:6) to afford 52 fractions. According to the TLC, fractions containing similar compounds were combined into 14 fractions, D1-D14; D1 (65 mg), D2 (196 mg), D3 (236 mg), D4 (205 mg), D5 (275 mg), D6 (224 mg), D7 (53.7 mg), D8 (182 mg), D9 (54 mg), D10 (67 mg), D11 (83 mg), D12 (57 mg), D13 (23 mg), D14 (13 mg). Fr. D3 (236 mg) was rich in **3** which was further applied to gel chromatography on a lipophilic Sephadex LH-20

column (25cm × 3cm) and using MeOH-H_2O mixture (1:1) to yield **3** (22 mg). D7 afforded **4** (53.7 mg). Additionally, Frs. D6 (224 mg), and D8 (182 mg) were also rich in **4**.

2.3.1.3. Isolation of neoclerodane-type diterpenoids, ***5*** *–* ***8***

Fractions E (Fr.10, 1.391 g) and F (Fr.11, 153 mg) were rich in lipophilic compounds which was further subjected to silica gel column (60 g) using a mixture of DCM-Aceton. An increasing amount of acetone in DCM in every 100 mL of the solvent mixture was applied [(stepwise gradient elution; 90:10 (400 mL), 85:15 (200 mL), 80:20 (300 mL)]. 76 Fractions were collected which were combined into 10 groups according to their TLC profiles (E1 – E10). Frs. E2 and E6 gave compounds **5** and **6**, (3 mg and 11 mg, resp.). Fr. E10 (74 mg) was further applied to a Sephadex LH-20 column (Ø 2 cm, h = 30 cm) using a mixture of Cyclohexane-Aceton-MeOH (7:2:1) to give **7** (25 mg) which was the major compound among the neo-clerodane type diterpenoids. Fr. F (fr. 11, 153 mg) was firstly applied to a silica gel column using DCM-MeOH-H_2O as mobile phase with increasing polarity (95:5:0.5→80:20:1). Fractions rich in compound **8** were further subjected to a Sephadex LH-20 column (Ø 2 cm, h = 30 cm) using a mixture of Cyclohexane-Acetone-MeOH (7:2:1) to give **8** (25 mg).

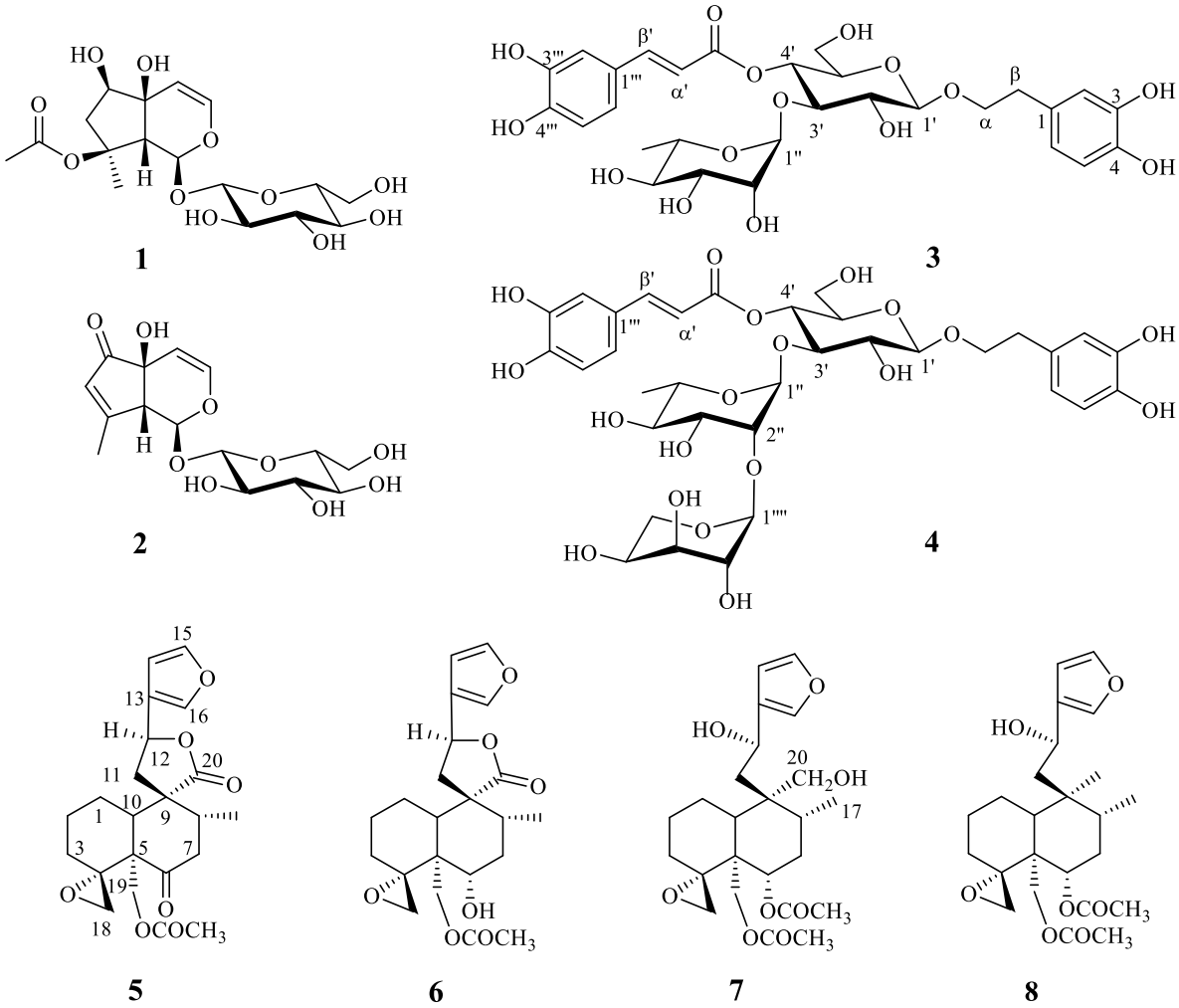

Figure 1. The structures of the compounds **1 – 8** isolated from *Teucrium creticum* L.

*8-O-Acetylharpagide (**1**)*: $[\alpha]_D^{20}$ -142.7° (c 0.22, MeOH); UV (MeOH) λ_{max} 211 nm; ^{1}H and ^{13}C NMR (CD_3OD) data, see Table 1.

*Teuhircoside (**2**)*: $[\alpha]_D^{20}$ -218.8° (c 0.16, MeOH); UV (MeOH) λ_{max} 228 and 210 (sh) nm; ^{1}H and ^{13}C NMR (CD_3OD) data, see Table 1.

*Verbascoside (= acteoside) (**3**)*: ^{1}H and ^{13}C NMR (CD_3OD) data, see Table 2.

*Lavandulifolioside (**4**)*: ^{1}H and ^{13}C NMR (CD_3OD) data, see Table 2.

*Teucrin H3 = 19-acetylgnaphalin (**5**)*: $[\alpha]_D^{20}$ +59.1° (c 0.115, $CHCl_3$); ^{1}H and ^{13}C NMR ($CDCl_3$) data, see Tables 3 and 4; (+)-HRMS m/z 425.1564 (100%) $[M+H]^+$, 827.3237 $[2M+H]^+$ (calcd. for $C_{22}H_{26}O_7Na$: 425.1576; Mol. wt. 402,1679).

*Teucjaponin B (**6**):* $[\alpha]_D^{20}$ +47.6 ° (c 0.084, $CHCl_3$); ^{1}H and ^{13}C NMR (CD_3OD) data, see Tables 3 and 4; (+)-HRMS m/z 405.1900 $[M+H]^+$, 427.1719 (87%) $[M+Na]^+$, 831.3549 $[2M+H]^+$ (calcd. for $C_{22}H_{28}O_7Na$: 427.1733; Mol. wt. 404.1835).

*Teucretol (**7**)*: $[\alpha]_D^{20}$ -12.7° (c 0.157, $CHCl_3$); ^{1}H and ^{13}C NMR (CD_3OD) data, see Tables 3 and 4; (+)-HRMS m/z 451.2321 (45%) $[M+H]^+$ 473.2136 (100%) $[M+Na]^+$ (calcd. for $C_{24}H_{34}O_8Na$: 473.2151; Mol. wt. 450.2254).

*Diacetylteumassulin (**8**)*: $[\alpha]_D^{20}$ -9.2° (c 0.35, $CHCl_3$); ^{1}H and ^{13}C NMR (CD_3OD) data, see Tables 3 and 4; (+)-HRMS m/z 435.2373 (30%) $[M+H]^+$ and 457.2191 (100%) $[M+Na]^+$ (calcd. for $C_{24}H_{34}O_7Na$: 457.2202; Mol. wt. 434.2305).

3. Results and Discussion

3.1. Structure Elucidation

Compound **1** was obtained as a colorless compound, $[\alpha]_D^{20}$ -142.7º (c= 0.22, MeOH). The UV (λ_{max} 211 nm, MeOH) and ^{1}H-NMR (δ 6.38 d, $J_{3,4}$= 6.4 Hz, H-3; 4.91 dd, $J_{4,3}$ = 6.4 and $J_{4.9}$ = 1.6 Hz, H-4) spectra of **1** indicated a non-conjugated iridoid enol-ether system (Table 1) indicating an aucubin-type iridoid structure. ^{13}C-NMR spectrum exhibited 17 carbon resonances; six of them were attributed to a β-D-glucopyranosyl unit while two of them were ascribed to the methyl and carbonyl carbons of an acetoxyl group. The remaining carbon resonances indicated that **1** has an iridoid (cyclopentanpyrane ring system) with nine carbon atoms. The complete assignments of all proton and carbon resonances were based on 2D-NMR (COSY, HSQC, HMBC and NOESY) experiments. The proton signals arising from an ABX system at δ 2.18 and 1.94 (each dd, J_{AB} 15.2 Hz, J_{AX} = 4.5 Hz, J_{BX} = 1.2 Hz, H_2-7; AB of ABX) and 3.71 (dd, J = 4.5 and 1.2 Hz, H-6; X of ABX) and the corresponding carbon resonances (δ 46.0 and 78.2) were assigned to H_2-7/C-7 and H-8/C-8, respectively. This statement was supported with the presence of two oxygen-bearing quaternary carbon resonances on both ends of this spin system ascertained as C-5 (δ 73.3) and C-8 (δ 88.6). The remaining proton signals at δ 6.08 (1H, d, $J_{1,9}$ = 1.2 Hz) 2.85 (1H, dd, $J_{9,1}$ = 1.2 Hz and $J_{9,4}$ = 1.6 Hz), 1.45 (3H, s) were determined as H-1, H-9 and H_3-10, respectively. The prominent HMBC correlations from C-1 to H-1', H-3 and H-9, from C-5 to H-1, H-3, H-9 and H-6, from C-9 to H-4, H-6 and H_2-7, and from C-8 to H-1, H-9, H_2-7 and H_3-10 supported the proposed structure for **1**. Moreover, the NOE between H-1/H_3-10 and H-7/H_3-10 indicated that these protons are on the same side (α) of the cyclopentanepyrane system confirming relative configuration. Additional NOE between H-1/H-1' supported the glycosidation site. The spectral data established the structure of **1** to be 8-*O*-acetylharpagide [15].

Compound **2** was obtained as a colorless compound, $[\alpha]_D^{20}$ -218.8º (c= 0.16, MeOH). The UV (λ_{max} 228 nm and 210 sh) and the ^{1}H-NMR spectrum of **2** [CD_3OD; δ 6.29 (d, $J_{3,4}$ = 6.4 Hz, H-3), 4.87 (dd, $J_{4,3}$ = 6.4, $J_{4,9}$ = 1.6 Hz, H- 4)], and 5.94 (q, H-7) indicated a non-conjugated iridoid enol-ether system and a conjugated enone system in a cyclopentane ring. The complete assignment of the 'H-

NMR spectrum is based on a homonuclear COSY experiment (Table 1). The starting point for the analysis of the iridoid protons is the *"d"* at 6.29 ppm (H- 3). It shows a correlation peak only with the *"dd"* at 4.87 ppm which confirms its assignment to H-4 which was further coupled to the *"m"* at 3.22 ppm (H-9) and *"br s"* at 2.23 ppm (3H), assigned to H_3-10. Moreover, H-9 shows correlations to both H_3-10 and to the *"d"* at 6.0 ppm ($J_{1,9}$ = 1.6 Hz, H-1). The olefinic proton signal observed at δ 5.94 (q) showed correlations to H_3-10 and H-9, was therefore assigned to H-7. This significant coupling pattern suggests a 7-ene-6-one structure, and the experimental results are also in good agreement with the reported data for allobetonicoside, teuhircoside and teucardoside with a similar iridoid skeleton [16-18].

The ^{13}C-NMR spectrum of **2** confirmed this assumption as the chemical shifts of the relevant iridoid C-atoms are similar to those of teuhircoside except small differences based on the solvent effect [16]. The signals observed at δ 174.7 and 206.8 were assigned to C-8 and C-6, respectively. The former showed the ^{13}C, ^{1}H-heteronuclear long-range correlations to H-1, H-9 and H_3-10 while the latter showed the correlations to H-4, H-7 and H_3-10.

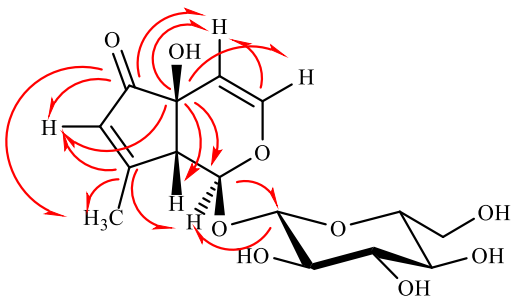

Figure 2. The significant ^{13}C,^{1}H-long-range Heteronuclear Correlations for **2**.

Table 1. ^{13}C ve ^{1}H NMR Data of 8-*O*-acetyl-harpagide (**1**) and Teuhircoside (**2**) (CD_3OD, * ^{13}C: 100 MHz; ^{1}H: 400 MHz)

C/H Atom	8-*O*-acetyl-harpagide (**1**)			Teuhircoside (**2**)		
	DEPT	δ_C ppm	δ_H ppm, *J* (Hz)	DEPT	δ_C ppm	δ_H ppm, *J* (Hz)
1	CH	94.5	6.08 d (1.2)	C	91.7	6.0 d (1.6)
3	CH	143.9	6.38 d (6.4)	CH	142.6	6.29 d (6.4)
4	CH	106.9	4.91 dd (6.4, 1.6)	CH	105.1	4.87 dd (6.4, 1.6)
5	C	73.3	-	CH	72.9	-
6	CH	78.2	3.71 dd (1.2, 4.5)	C	206.8	-
7	CH_2	46.0	2.18 dd (15.2, 1.2) 1.94 dd (15.2, 4.5)	CH	128.8	5.94 qui
8	C	88.6	-	C	174.7	-
9	CH	55.4	2.85 br s	CH	58.0	3.22†
10	CH_3	22.5	1.45 s	CH_3	17.9	2.23 br s
*C*OCH$_3$	C	173.3	-			
CO*CH$_3$*	CH_3	22.2	2.01 s			
Glucose						
1'	CH	99.9	4.58 d (8.0)	CH	99.1	4.55 d (8.0)
2'	CH	74.6	3.19 dd (8.0, 9.2)	CH	75.1	3.21 dd (8.0, 9.2)
3'	CH	77.5	3.38 t (9.2)	CH	77.5	3.38 t (9.0)
4'	CH	71.7	3.43 t (9.0)	CH	71.7	3.27 t (9.0)
5'	CH	77.6	3.64 – 3.50†	CH	78.5	3.30†
6'	CH_2	62.8	3.88 dd (12.4, 1.6) 3.68 dd (12.4, 5.6)	CH_2	62.8	3.92 dd (12.0, 2.2) 3.66 dd (12.0, 6.0

The assignments are based on 2D NMR experiments (COSY, HSQC and HMBC)
†The signal pattern is unclear due to overlapping.

These observations confirmed the suggested iridoid skeleton exhibiting a 7-ene-6-one structure for **2**. The second spin system observed in the COSY experiment and corresponding carbon resonances assigned by the help of HSQC experiment allowed the presence of a β-D-glucopyranose unit. The glycosidation site was determined by the help of HMBC (Figure 2), which showed the ^{13}C,^{1}H-heteronuclear long-range correlation from C-1 (δ 91.7) to the anomeric proton of D-glucose (δ 4.55, d, J = 8.0 Hz, H-1') and the vice versa correlation from the anomeric carbon of the glucose (δ 99.1, C-1') to H-1 of the iridoid moiety (δ 6.0, d, *J* = 1.6 Hz). Furthermore, C-1 showed the long-range correlations to H-3, H-7 and H-9. Based on these observations, compound **2** was identified as teuhircoside [17].

Table 2. ^{13}C ve ^{1}H NMR Data of Verbascoside (**3**) and Lavandulifolioside (**4**)*

		3		**4**	
C/H Atom		δ_C ppm	δ_H ppm, *J* (Hz)	δ_C ppm	δ_H ppm, *J* (Hz)
Aglycone 1	C	131.5		131.4	
2	CH	117.1	6.68 d (2.0)	117.1	6.69 d (2.0)
3	C	146.1		146.1	
4	C	144.7		144.7	
5	CH	116.3	6.55 dd (2.0, 8.0)	116.3	6.56 dd (2.0, 8.0)
6	CH	121.2	6.66 d (8.0)	121.3	6.67 d (8.0)
α	CH_2	72.3	4.04 m, 3.71 m	72.3	4.05 m, 3.70 m
β	CH_2	36.6	2.79 brt (7.4)	36.6	2.79 t (7.4)
Glucose 1'	CH	104.2	4.37 d (8.0)	104.2	4.37 d (8.0)
2'	CH	76.2	3.38 dd (8.0, 9.2)	76.0	3.38 dd (8.0, 9.2)
3'	CH	81.6	3.81 t (9.2)	82.4	3.75 – 3.80†
4'	CH	70.4	4.90 t (9.0)	70.4	4.92†
5'	CH	76.0	3.64 – 3.50†	76.0	3.50 – 3.60†
6'	CH_2	62.4	3.64 – 3.50†	62.3	3.60 – 3.66†
Rhamnose 1"	CH	103.0	5.18 d (1.6)	102.0	5.49 d (1.6)
2"	CH	72.3	3.91 dd (1.6, 3.2)	82.9	3.94 dd (1.6, 3.2)
3"	CH	72.1	3.56 dd (3.2, 9.6)	72.3	3.49 dd (3.2, 9.6)
4"	CH	73.8	3.28 t (9.6)	74.2	3.27 t (9.6)
5"	CH	70.6	3.60 m	70.6	3.50 – 3.60†
6"	CH_3	18.5	1.08 d (6.0)	18.4	1.05 d (6.0)
Arabinose 1""	CH			107.5	4.30 d (7.0)
2""	CH			72.8	3.60 – 3.66†
3""	CH			74.4	3.48 – 3.56†
4""	CH			69.9	3.74 – 3.80†
5""	CH_2			67.3	3.85 dd (12.8, 2.8)
					3.48 – 3.56†
Caffeoyl 1'''	C	127.6		127.6	
2'''	CH	115.2	7.04 d (2.0)	115.2	7.05 d (2.0)
3'''	C	146.9		146.8	
4'''	C	149.9		149.8	
5'''	CH	116.5	6.94 dd (2.0, 8.0)	116.5	6.95 dd (2.0, 8.0)
6'''	CH	123.2	6.76 d (8.0)	123.2	6.77 d (8.0)
α'	CH	114.7	6.27 d (15.6)	114.6	6.27 d (15.6)
β'	CH	148.0	7.59 d (15.6)	148.0	7.60 d (15.6)
C=O	C	168.3		168.3	

(*CD_3OD, ^{13}C: 100 MHz; ^{1}H: 400 MHz).
†Signal pattern unclear due to overlapping.

Compounds **3** and **4** were obtained as pale yellow, amorphous compounds. The ^{1}H NMR spectra of **3** and **4** (see Table 2) exhibited the protons of two aromatic rings as ABX systems which were characteristic for (*E*)-caffeic acid and 3,4-dihydroxyphenylethanol moieties (H-2, H-5 and H-6 of 3,4-dihydroxyphenetyl moiety and H-2''', H-5''' and H-6''' of. Additionally, two *trans*-olefinic protons as an

AB system (J_{AB}= 15.6 Hz, H-α' and H-β'), a benzylic *β*-methylene protons at δ 2.79 (2H, br t, *J* =7.4 Hz, H_2-β), and two nonequivalent hydroxymethylene protons at δ 4.04/4.05 and 3.70/3.71 (each 1H, m, H_2-α) of the side-chain of the aglycon moiety were observed as the common signals of **3** and **4**. The ^{13}C NMR spectra of **3** and **4** were consistent for the presence of a caffeic acid, 3,4-dihydroxyphenyl ethanol and di- and triglycosidic sugar moieties characteristic for the phenylethanoid glycosides except the number of anomeric proton signals. The ^{1}H-NMR spectrum of **3** indicated a diglycosidic structure consisting of a hexose and methylpentose = 6-deoxy-hexose (δ 4.37, d, *J* = 8.0 Hz, H-1' of β-D-glucose; δ 5.18, d, *J* = 1.6 Hz, H-1" of α-L-rhamnose). The glycosidation shift observed in ^{13}C-NMR experiment for C-3' of glucose (δ 81.6) and the downfield shift observed for H-4' of glucose moiety (δ 4.90 t, J = 9.0 Hz) clearly supported the structure of compound **3** as verbascoside (= acteoside) [19]. The ^{1}H- and ^{13}C-NMR spectra of **4** indicated a triglycosidic structure consisting of a hexose, a methylpentose and a pentose (δ 4.37, d, *J* = 8.0 Hz, H-1' of β-D-glucose; δ 5.49, d, *J* = 1.6 Hz, H-1" of α-L-rhamnose; δ 4.30, d, *J* = 7.0 Hz, H-1"" of α-L-arabinose) units. The corresponding carbon resonances of the arabinose unit indicated its terminal position. Additional glycosidation shift observed for C-2" of rhamnose unit (δ 82.9) which pointed out the glycosidation site of the third sugar, arabinose on the rhamnose unit to be C-2(OH). This suggestion was supported by the +0.30 ppm down-field shift of the anomeric proton resonance of α-L-rhamnose unit (δ 5.49, d, *J* = 1.6 Hz, H-1") substituted at C-2"(OH) in comparison to those of verbascoside (δ 5.18, H-1"). Based on the ^{1}H- and ^{13}C-NMR data, the structure of **4** determined as lavandulifolioside which was firstly reported from *Stachys lavandulifolia* [20].

Compound **5** was obtained as a white amorphous compound. The positive ion HR-MS of **5** gave a quasimolecular ion $[M+Na]^+$ peaks at m/z 425,1564 compatible with the molecular formula of $C_{22}H_{26}O_7Na$ (Mr of 425,1576) and 10 degrees of unsaturation. This result indicated that the molecular weight of **5** is to be 402,1679 ($C_{22}H_{26}O_7$).

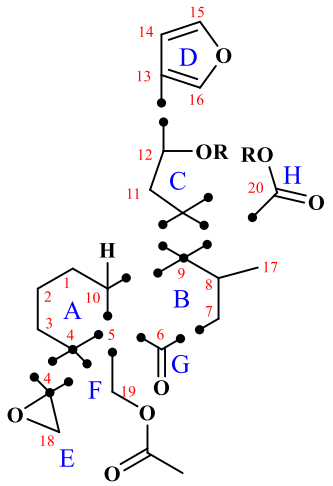

Figure 3. Molecular fragments of compound **5** deduced from 2D-NMR experiments

The ^{13}C-NMR of **5** displayed the 22 carbon resonances due to a methyl, an acetoxy methyl, seven methylene (two oxygenated), six methine (one oxygenated and three olefinic), and seven quaternary (two oxygenated, one olefinic, and three carbonyl) carbon atoms (Table 4). The assignments of all proton signals were based on a COSY experiment (Table 3). After assigning of the proton signals, the corresponding carbon resonances were established via ^{13}C – ^{1}H shift-correlated one-bond (HSQC) experiment. Thus, eight molecular fragments (A – H) were established (Figure 3). The ^{1}H-NMR spectrum of **5** revealed the proton signals assigned to three methylene resonances belonging to the A ring (H_2-1, H_2-2 and H_2-3) which were observed in the same spin system. Additionally, a methine signal at δ 2.05 (1H, dd, J = 13.4 and 3.7 Hz, H-10) was found to be part of this spin network (fragment A). A secondary methyl resonance (Me-17) was observed in the same spin system with the proton at δ 1.94 (1H, H-8) and the methylene protons at δ 3.47 (t, *J* = 13.5 Hz, H-7a) and 2.08 (dd, *J* = 13.5 and 3.8 Hz, H-7b) (fragment B). A proton signal at δ 5.39 (t, *J* = 9.6 Hz, H-12)

and two protons at δ 2.38 (2H, dd, J = 8.5 Hz, H_2-11) were observed as an ABX system. This molecular fragment (-CH_2-CHX-O-) supported the presence of a γ-spirolactone moiety (fragment C). Three protons at δ 6.31, 7.36 and 7.37 (each 1H, br s, H-14, H-15, and H-16) in the same spin system were consistent for the presence of β-substituted furan ring (fragment D). The remaining signals were attributed to two epoxide protons as an AX system (δ 3.51 and 2.19, J_{AX} = 5.7 Hz, H_2-18) of an oxirane, two downfield-shifted oxymethylene protons as an AB system (δ 5.40 and 4.99, J_{AB} = 13.0 Hz, H_2-19) with an acetoxyl group (δ 2.01 s) which were assigned to the molecular fragments E and F, respectively. The ^{13}C-NMR spectrum additionally indicated the presence of three carbonyl fuctionalities at δ 207.1 (C-6), 176.6 (C-20) (fragments G and H, resp.) and 170.1 (*C*OCH_3). Three carbonyl resonances and two endocyclic double bonds of the furan ring clearly suggested the presence of a pentacyclic structure for **5**. Intermolecular connectivities were established by the help of a long-range ^{13}C – ^{1}H heteronuclear correlation (HMBC) experiment (Figure 4). The long-range correlations from C-5 to H_2-18, H_2-19, and from C-4 and C-6 to H_2-19, as well as from C-9, C-10, and C-29 to H_2-11, generated the A and B fragments of a decalin moiety which bears an oxirane (C-18) at C-4, acylated hydroxymethylene (C-19) at C-5, and a γ-spirolactone moieties at C-9. (fragments E, F and C, respectively). Furthermore, the long-range correlations from C-13 to H-16 and H-12 were evident for the location of the furan ring. The core decalin moiety in clerodane-type diterpenoids consisting of a 5:10 *trans* ring junction is characteristic for the family Lamiaceae [21] and *Teucrium* species [5]. This data was in good agreement with those reported for a clerodane-type diterpene, teucrin H3 [19-acetoxy-4α,18:15,16-diepoxy-6-keto-neo-cleroda-13(16),14-dien-20,12*S*-olide] isolated from *T. hyrcanicum* [22]. Teucrin H3 was also reported from *T. gnapholides* and named as 19-acetylgnaphalin [23]. Malakov and his friends (1979) reported this diterpenoid from *T. polium* using both trivial names, teucrin H3 and 19-acetylgnaphalin Based on these results, the structure of **5** was established as teucrin H3 [24].

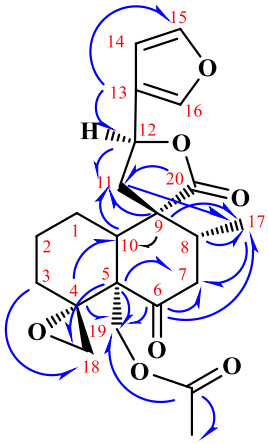

Figure 4. The significant ^{13}C – ^{1}H long-range heteronuclear correlations observed for **5**

Compound **6** {$[\alpha]_D^{20}$ +47.6° (c= 0.084, $CHCl_3$)} had the molecular formula $C_{22}H_{28}O_7$ as determined by the positive ion HR-MS which exhibited a quasimolecular ion $[M+Na]^+$ peak at m/z 427,1719 which corresponds with the molecular formula $C_{22}H_{28}O_7Na$ with a Mr of 427,1733 and 9 degrees of unsaturation. This result indicated the molecular weight of **6** to be 404,1835 ($C_{22}H_{28}O_7$). The difference in molecular weight between the compounds **5** and **6** is two daltons. The ^{1}H-NMR spectrum of **6** revealed a secondary methyl (δ 0.95 d, J = 6.5 Hz, Me-17), an acetoxyl group (δ 2.01 s), a geminal proton of a hydroxyl group (δ 3.59 dd, J = 12.7 and 2.8 Hz, H-6), two epoxide protons as an AX system (δ 3.16 and 2.40, J_{AX} = 2.8 Hz, H_2-18), and two oxymethylene protons as an AB system (δ 4.94 and 4.64, J_{AB} = 13.1 Hz, H_2-19). A proton signal at δ 5.28 (t, J = 8.5 Hz, H-12) and two protons at δ 2.29 (2H, br d, J = 8.5 Hz, H_2-11) were observed in the same spin system. Three protons at δ 6.31, 7.36 and 7.37 (each 1H, br s, H-14, H-15 and H-16) in the same spin system were consistent for the

presence of β-substituted furan ring. The difference between **5** and **6** was due to proton and carbon resonances arising from the molecular fragment B. Compound **6** was found to have a hydroxyl group at C-6 (δ 3.59) instead of a ketone function of **5**. NMR data of **6** (Tables 3 and 4) was in good accordance with those reported for teucjaponin B, a (12*S*)-neoclerodan-20,12-olide-type diterpenoid [25]. Moreover, in the NOESY experiment performed with **5** and **6**, the lack of NOE-cross-peaks between H_3-17/H-12 supported the C-12(*S*) configuration for both [26]. Consequently, the structure of **6** was identified as 19-acetoxy-4α,18:15,16-diepoxy-6α-hydroxy-*neo*-cleroda-13(16),14-diene-20,12(*S*)-olide.

Table 3. ^{1}H-NMR data for diterpenoids, **5 – 8**

	5	**6**	**7**	**8**
C/H	**δ_H ppm, *J* (Hz)**	**δ_H ppm, J (Hz)**	**δ_H ppm, J (Hz)**	**δ_H ppm, J (Hz)**
1a	1.85 brd,	1.82 brd (12.0)	2.03†	2.03 m
1b	1.71 ddd	1.68 dd (12.0, 3.6)	1.73†	1.54 m
2a	1.97 m	1.99†	1.90 m	1.92 m
2b	1.47 m	1.45†	1.42 m	1.50 m
3a	2.43 m	2.17 ddd “bt” (12.8)	2.10†	2.15 m
3b	0.94 m	1.04 brd (12.8)	1.04 brd (12.9)	1.05 m
6	-	3.59 dd (12.7, 2.8)	4.74 dd (10.6, 5.0)	4.76 dd (12.1, 4.8)
7a	3.47 t (13.5)	2.08 ddd (15.3, 12.7)	1.73†	1.63 m
7b	2.08 dd (13.5, 3.8)	1.60 dt (12.7, 12.7, 2.3)	1.52 ddd (9.5, 9,5, 4.3)	1.51 m
8	1.94†	1.54 m	1.73†	1.78 m
10	2.05 dd (13.4, 3.7)	1.59 †	1.98 dd (12.3, 2.3)	2.02 dd (13.0, 3.0)
11a	2.38 dd (8.5, 5.7)	2.29 brd (8.5)	2.14 dd (15.8, 7.0)	1.94†
11b			1.79 dd (15.8, 2.2)	1.60 dd (16.0, 2.3)
12	5.39 t (8.6)	5.28 t (8.5)	4.86 dd (8.9, 2.0)	4.79 dd (8.9, 2.3)
14	6.32 brs	6.31 brs	6.41 t (1.2)	6.39 d (1.5)
15	7.40 brs	7.36 †	7.39†	7.39 t (1.5)
16	7.38 brs	7.37 †	7.39†	7.37 brs
17	1.00 d (6.7)	0.95 d (6.5)	0.92 d (6.2)	0.78 d (6.7)
18a	3.51 d (5.7)	3.16 d (2.8)	3.01 dd (4.0, 2.2)	3.01 dd (4.0, 2.4)
18b	2.19 d (5.7)	2.40 d (2.8)	2.21 d (4.0)	2.22 d (4.0)
19a	5.40 d (13.0)	4.94d (13.1)	4.89 d (12.0)	4.86 d (12.1)
19b	4.99 d (13.0)	4.64 (13.1)	4.42 d (12.0)	4.39 d (12.1)
20	-	-	3.59 brs	0.71 s
CO<u>C</u>H$_3$	2.01 s	2.01 s	2.10 s	2.10
CO<u>C</u>H$_3$			1.94 s	1.95

*All assignments are based on 2D-NMR experiments (COSY, HSQC and HMBC). (□$_H$: 500 MHz, $CDCl_3$).
† Signal pattern unclear due to overlapping

Compound **7** had the molecular formula $C_{24}H_{34}O_8$, as determined by HR-MS. The positive-ion HR-MS showed a quasimolecular ion peak at m/z 473,2136 $[M+Na]^+$ (calc. for $C_{24}H_{34}O_8Na$), corresponding to the molecular formula $C_{24}H_{34}O_8$ (Mr of 450,2254) and 8 degrees of unsaturation. The assignment of all proton and carbon resonances were based on 2D-NMR (COSY, HSQC and HMBC) experiments which were characteristic for furanoid diterpene such as **5** and **6** (Tables 3 and 4). Two carbonyl resonances and two endocyclic double bonds of the furan ring clearly suggested the presence of a tetracyclic structure for **7**. In the ^{1}H-NMR spectrum of **7**, a secondary methyl (δ 0.92, d, *J* = 6.2

Hz, H_3-17), two acetoxymethyl (δ 1.94 and 2.10, each 3H, s), two protons as an AX system of the oxirane ring (δ 3.01 and 2.21, both d, J_{AX} = 4.0 Hz, H_2-18), a broad singlet with two proton intensity of a hydroxymethylene signal (δ 3.59, H_2-20), two protons as an AB system (δ 4.89 and 4.42, both d, J_{AB} = 12.0 Hz, H_2-19) and an oxymethine proton (δ 4.74, dd, J = 10.6 and 5.0 Hz) were clearly observed. The remaining signals were arising from an ABX system at δ 2.14, 1.79 (each 1H, each dd, H_2-11) and 4.86 (1H, dd, H-12). By the help of an HMBC experiment, intermolecular connectivites were established (Figure 5). NOESY spectrum showed the cross-peaks between H_2-19/H_2-20 and H_2-19/H_3-17 indicating that these protons were the same side of the decaline moiety. On the other hand, the nOe correlations observed between the H_2-18/H-6 and H-6/H-10 indicated that these protons were on the reverse side of the *trans*-decaline ring. These observations and full NMR data and the optical rotation value {$[\alpha]_D^{20}$ -8.8° (c= 0.157, $CHCl_3$)} were in superimposable in accordance with those reported for teucretol [6α,19-diacetoxy-4α,18:15,16-diepoxy-12*S*,20-dihydroxy-*neo*-cleroda-13(16),14diene] isolated from the same plant, *Teucrium creticum* collected from (Cyprus) [27].

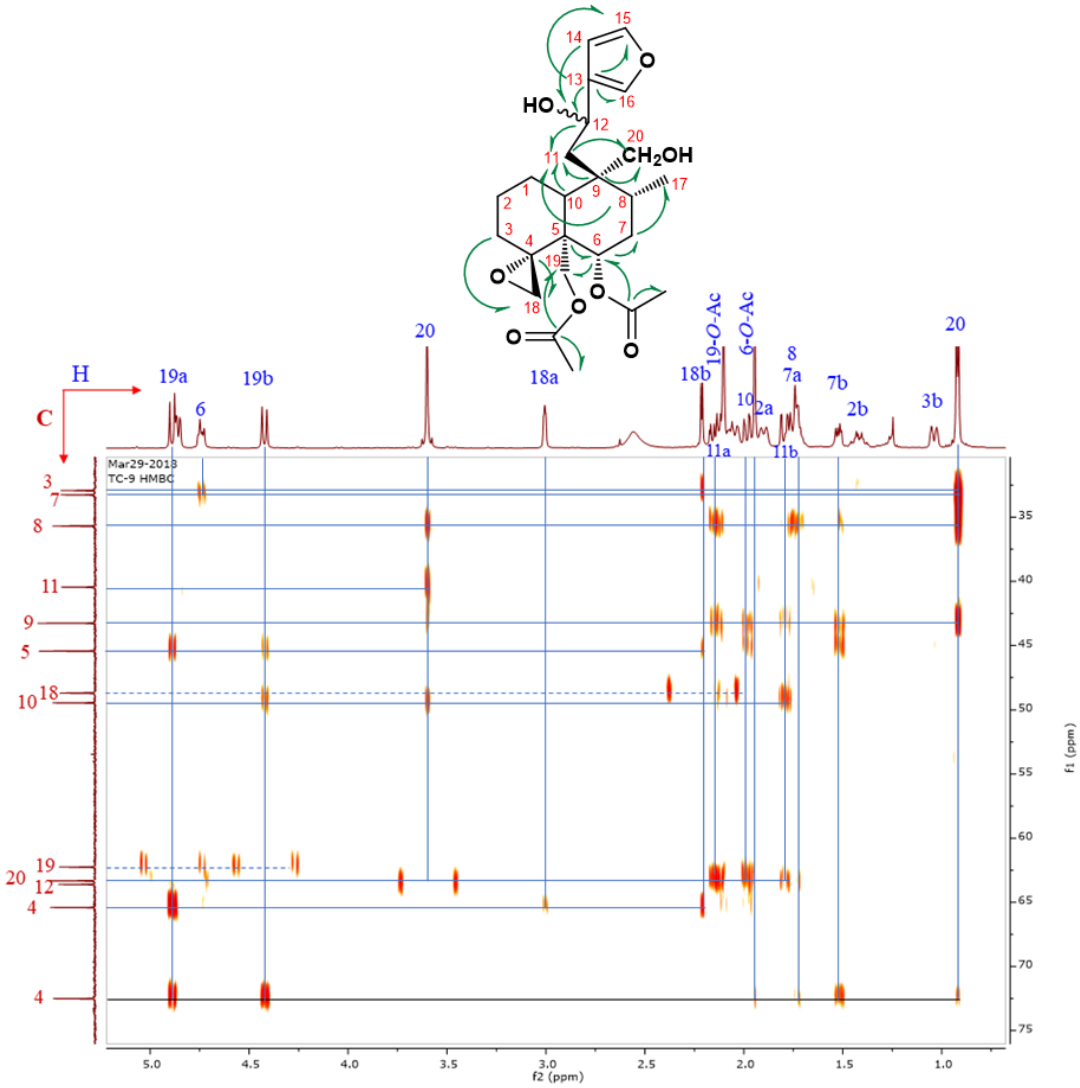

Figure 5. The Significant ^{13}C-^{1}H Long-range heteronuclear correlations (HMBC) observed for **7** (^{1}H: 0.50 – 5.25 ppm; ^{13}C: 30 – 75 ppm)

Compound **8** gave a a quasimolecular ion peak in its positive-ion HR-MS at m/z 457,2191 $[M+Na]^+$ (calc. for $C_{24}H_{34}O_7Na$), corresponding to the molecular formula $C_{24}H_{34}O_7$ (Mr of 457,2202) and 8 degrees of unsaturation. The ^{13}C NMR spectrum displayed 22 signals due to four methyl (one

secondary methyl, one tertiary methyl and two acetoxymethyl), six methylenes (two oxygenated), seven methine (one oxygenated, three olefinic) and five quaternary (two oxygenated, one olefinic, two carbonyl) carbon atoms (Table 1). This data was indicative for a tetracyclic structure for **8**. The ^{1}H-NMR spectrum of **8** showed the presence of three olefinic protons, four methyl resonances (one secondary, one tertiary and two acetoxy) and a pair of two hydroxymethylene signals which were very similar to those observed for **7** except the presence of a tertiary methyl resonance (δ 0.71 s, H_3-20) and the lack of hydroxymethylene resonance assigned as H_2-20. The 2D-NMR experiments (COSY, HSQC, HMBC and NOESY) pointed out the two of four rings were arising from the *trans*-decalin moiety, the third one belonged the oxirane ring and the last one was due to the furan ring. These molecular fragments were clearly assembled into the basic framework of **8** from the results of the HMBC experiment. The relative stereochemistry of the oxirane ring, acetylated hydroxymethylene and hydroxymethine functionalities, the tertiary and secondary methyl groups was established by the help of NOESY experiment. All these data as well as optical rotation value {$[\alpha]_D^{20}$ -9.2 (c. 0.348, $CHCl_3$)} suggested that the compound **8** is 6,19-diacetylteumassilin [6α,19-diacetoxy-4α,18:15,16-diepoxy-12*S*-hydroxy-*neo*-cleroda-13(16),14diene] isolated from *Teucrium massilense* [28].

Table 4. ^{13}C-NMR data for diterpenoids, **5 – 8**

	5		**6**		**7**		**8**	
C/H	**DEPT**	**δ_C ppm**	**DEPT**	**δ_C ppm**	**DEPT**	**δ_C ppm**	**DEPT**	**δ_C ppm**
1	CH_2	23.5	CH_2	22.6	CH_2	22.7	CH_2	21.5
2	CH_2	24.8	CH_2	25.0	CH_2	25.2	CH_2	24.8
3	CH_2	32.8	CH_2	31.3	CH_2	32.9	CH_2	32.8
4	C	54.2	C	66.6	C	65.4	C	65.2
5	C	61.3	C	45.3	C	45.4	C	45.5
6	C	207.1	CH	73.4	CH	72.5	CH	72.5
7	CH_2	43.5	CH_2	33.8	CH_2	33.3	CH_2	33.0
8	CH	41.6	CH	38.3	CH	35.7	CH	35.1
9	C	51.7	C	51.1	C	43.3	C	39.0
10	CH	55.6	CH	52.4	CH	49.5	CH	48.6
11	CH_2	43.7	CH_2	43.5	CH_2	40.5	CH_2	44.8
12	CH	72.0	CH	71.5	CH	63.3	CH	63.0
13	C	124.9	C	125.1	C	130.8	C	131.0
14	CH	107.9	CH	108.0	CH	108.4	CH	108.3
15	CH	139.6	CH	144.2	CH	143.6	CH	143.6
16	CH	144.4	CH	139.6	CH	138.4	CH	138.3
17	CH_3	17.1	CH_3	16.5	CH_3	16.9	CH_3	15.5
18	CH_2	48.6	CH_2	48.5	CH_2	48.7	CH_2	48.5
19	CH_2	62.1	CH_2	61.7	CH_2	62.3	CH_2	61.9
20	C	176.6	C	176.0	CH_2	63.6	CH_3	17.3
$\underline{C}OCH_3$	C	170.8	C	170.7	C	170.3	C	170.1
$CO\underline{C}H_3$	CH_3	20.9	CH_3	21.3	CH_3	21.3	CH_3	21.3
$\underline{C}OCH_3$					C	170.1	C	170.0
$CO\underline{C}H_3$					CH_3	21.2	CH_3	21.2

*δ_H: 125 MHz, $CDCl_3$.

4. Conclusion

Present study resulted in the isolation of two iridoids which are 8-*O*-acetylharpagide (**1**) and teuhircoside (**2**); in addition to two phenylethanoid glycosides which are verbascoside (**3**) and lavandulifolioside (**4**), and finally four neoclerodane-type diterpenoids; teucrin H3 (= 19-acetylgnaphalin) (**5**), teucjaponin B (**6**), teucretol (**7**), and diacetylteumassilin (**10**). All findings are isolated from *T. creticum* (Section: Teucrium): which is named as "*Girit Kurtlucası*" in Turkish [29].

First of all with regards to iridoids; previous research reports limited structural diversity of the iridoids in *Teucrium* species. [30-35]. In this respect it is important to note that within this recent study, a potential active metabolite group of iridoids are isolated.which are harpagide, 8-*O*-acetylharpagide, teuhircoside and teucardoside.

Secondly, with regards to the phenylethanoid glycosides, acteoside (**3**) and lavandulifolioside (**4**) were isolated. As a diglycoside, acteoside (**3**) is the predominant compound in plants rich in phenylethanoid glycosides. Lavandulifolioside (**4**) has a triglycosidic structure similar poluimoside [9, 36], and teucrioside [10, 37, 38] which were reported from other *T. polium* (Section: Polium) and *T. chamaedrys* (Section: Chamaedrys), respectively. Interestingly, the glycosidation pattern of lavandulifolioside shows similarity to those of teucrioside. The third sugar on the rhamnose unit of acteoside is xylose for lavandulifolioside while it is a rare sugar lyxose for teucrioside. In previous researche, a series of pharmacological and biological activities of many medicinal plants have been ascribed to the presence of phenylethanoid glycosides [39-42]. In addition, a recent study reported the neuroprotective actions of echinacoside as a potential therapeutic agent for preventing the progression of Alzheimer disease [43]. Phenylethanoid (phenylpropanoid) glycosides as caffeoyl sugar esters are found in many gamopetalous plants [44]. In chemotaxonomical studies, the subfamily division of the Lamiaceae has been based on two chemical characteristics, which are rosmarinic acid and caffeic acid sugar esters, or, phenylethanoid glycosides [45].

Finally, in this study diterpenoids: **5-8** were isolated from *T. creticum*. They exhibit neo-clerodane skeleton. Diterpenoids from the *Teucrium* species exhibit neo-clerodane skeleton, which are chemotaxonomic markers, and, isolated from the aerial parts of plants [5, 21]. As documented by previous research, rearranged abietane-type diterpenes are isolated from the roots of *Teucrium* species. Some neo-clerodane diterpenoids, especially furan-containing diterpenoids, are highly hepatotoxic causing hepatic necrosis in mice. They have also been thought to cause, or provoke chronic hepatitis, or and cirrhosis in humans [21, 46, 47]. Current research on the genus also reported hepatotoxicity and, biological activity [48], as well as diterpenoids [49] performed on the *Teucrium* species.

Former studies conducted on different *Teucrium* species report flavonoids, as other phenolic metabolites, sesquiterpenes, triterpenes steroids, as well as monoterpenes as the constituents of volatile oils, have been reported. Flavonoids are mostly apigenin and luteolin type flavones, quercetin type flavonols and their 6-OH or 8-OH derivatives and glycosides. Most of the flavon and flavonol are methoxylated [50, 51]. Many activities such as antioxidant, antiinflammatory and antirheumatic, antihistaminic, spasmolitic, antigonadotropic, vasodilatory, sucrase inhibitory, inhibitory, DNA polymerase, hepatoprotective, antimicrobial, antiallergic are attributed to the flavonoids of *Teucrium* species [51]. Linalool, β-caryophyllene and caryophyllene oxide and spathulenol were found as major constituents of flower, leaf and fruit oils of *T. creticum* collected from Cyprus [52]. A recent study has reported the significant antimicrobial activity of aqueous and methanolic extracts of the leaves of *T. creticum* against eight multidrug-resistant bacteria isolated at an oncology department and reference bacterial and fungal strains [53].

Having said that, as a final remark, it is important to recall that the consumption of herbal products, in this case of *Teucrium* species, needs further attention due to the potential toxic metabolites, in spite of the presence of highly effective metabolites such as isoprenoids, flavonoids and phenylethanoid glycosides.

Acknowledgements

The authors kindly thank Anzarul Haque for 1D and 2D NMR measurements of the diterpenoids and Ayman Salkini for HRMS (Prince Sattam Bin Abdulaziz University, Saudi Arabia).

The authors also thank to Prof. Dr. Hakan Gögen (Ankara University, Faculty of Pharmacy, Ankara, Turkey) for the1D and 2D NMR measurements of the iridoids and phenylethanoid glycosides.

Supporting Information

Supporting information accompanies this paper on http://www.acgpubs.org/journal/records-of-natural-products

ORCID
Azmi Hanoğlu: 0000-0002-7586-9080
Duygu Yiğit Hanoğlu: 0000-0003-1345-4768
Nilay Demirel: 0000-0002-9262-099X
Hasan Soliman Yusufoğlu: 0000-0001-7062-8029
İhsan Çalış: 0000-0001-5489-3420

References

[1] F. Celep and T. Dirmenci (2017). Systematic and biogeographic overview of *Lamiaceae* in Turkey, *Nat. Vol. Essent. Oils.* **4**, 14-27.

[2] B. Li, P.D. Cantino, R.G. Olmstead, G.L.C. Bramley, C.L. Xiang, Z.H. Ma, Y.H. Tan and D.X. Zhang (2016). A large-scale chloroplast phylogeny of the *Lamiaceae* sheds new light on its subfamilial classification, *Sci. Rep.* **6,** 1–18.

[3] R.D. Meikle (1985). Flora of cyprus. The bentham-moxon trust, royal botanic gardens, kew, 2, 833-1969. ISBN 0 9504876 43, Clark Constable, Edinburgh, London, Melbourne.

[4] J. Jakupovic, R. N. Baruah, F. Bohlmann and W. Quack (1985). New clerodane derivatives from *Teucrium scordium*, *Planta Med.* 341- 342.

[5] A. Ulubelen, G. Topçu and U. Sönmez (2000). Chemical and biological evaluation of genus *Teucrium*. In: Studies in Natural Products Chemistry, *ed*: Atta-ur Rahman, Elsevier Science, Amsterdam, Netherlands, Vol.23, *pp* 591 – 648.

[6] N.A. Bukhari, R.A. Al-Otaibi and M. M. Ibhrahim (2015). Biodiversity characteristics of *Teucrium Polium* species in Saudi Arabia, *Saudi J. Biol. Sci.* **22**, 181-185.

[7] N.A. Jaradat (2015). Review of the taxonomy, ethnobotany, phytochemistry, phytotherapy and phytotoxicity of germander plant (*Teucrium polium* L.), *Asian J. Pharm. Clin. Res.* **8**, 13-19.

[8] Z. Yaniv, A. Dafni, J. Friedman and D. Palevitch (1987). Plants used for the treatment of diabetes in Israel, *J. Ethnopharmacol*. **19**: 145-151.

[9] C. Andary, R. Wylde, A. Heitz, J.P. Rascol, J.L. Roussel and C. Laffite (1985). Poliumoside, a caffeic glycoside ester from *Teucrium belion*, *Phytochemistry* **24**, 362-364.

[10] G.A. Gross, M.F. Lahloub, C. Anklin, H.-R. Schulten and O. Sticher (1988). Teucrioside, a phenylpropanoid glycoside from *Teucrium Chamaedrys*, *Phytochemistry* **27**, 1459-1463.

[11] F. Antognoni, C. Iannello, M. Mandrone, M. Scognamiglio, A. Fiorentino, P.P. Giovannini and F. Poli (2012). Elicited *Teucrium chamaedrys* cell cultures produce high amounts of teucrioside, but not the hepatotoxic neo-clerodane diterpenoids, *Phytochemistry* **81**, 50-59.

[12] S. Pacifico, B. D'Abrosca, M. Scognamiglio, G. D'Angelo, M. Gallicchio, S. Galasso, P. Monaco and A. Fiorentino (2012). NMR-based metabolic profiling and in vitro antioxidant and hepatotoxic assessment of partially fractions from golden germander (*Teucrium polium* L.) methanolic extract, *Food Chem*, **135**, 1957-1967.

[13] M. Bruno, S. Rosselli, A. Maggio, F. Piozzi, L. Scaglioni, N.A. Arnold and M.S.J. Simmonds (2004). Neoclerodanes from *Teucrium orientale*, *Chem. Pharm. Bull.* **52**, 1497-1500.

[14] M.S. Stankovic, M.G. Curcic, J.B. Zizic, M.D. Topuzovic, S.R. Solujic and S.D. Markovic (2011). *Teucrium* plant species as natural sources of novel anticancer compounds: Antiproliferative, proapoptotoic and antioxidant properties, *Int. J. Mol. Sci.* **12**, 4190-4205.

[15] Y. Takeda, S. Tsuchida and T. Fujita (1987). Four new iridoid glucoside *p*-Coumaroyl esters from *Ajuga decumbens*, *Phytochemistry* **26**, 2303-2306.

[16] M. Jeker, O. Sticher, İ. Çalış and P. Rüedi (1989). Allobetonicoside and 6-*O*-Acetylmioporoside from *Betonica officinalis* L., *Helv. Chim. Acta*. **72**, 1787-1791.

[17] J. Ruhdorfer and H. Rimpler (1981). Iridoide aus einigen *Teucrium*- und *Ajuga*-Arten, *Z. Naturforsch. C*. **36,** 697-707.

[18] J. Ruhdorfer and H. Rimpler (1981). Teucardosid, ein neues iridoid aus *Teucrium arduini* L. und *Teucrium hircanicum* L., *Tetrahedron Lett.* **22**, 839-842.

[19] O. Sticher and M. F. Lahloub (1982). Phenolic glycosides of *Paulownia tomentosa* bark, *Planta Med.* **46**, 145-148.

[20] A.A. Başaran, İ. Çalış, C. Anklin, S. Nishibe and O. Sticher (1988). Lavandulifolioside: A new phenylprophanoid glycoside from *Stachys lavandulifolia, Hel. Chim. Acta* **71**, 1483-1490.

[21] R. Li, S. L. Morris-Natschkeb and K. H. Lee (2016). Clerodane diterpenes: Sources, structures and biological activities, *Nat. Prod Rep.* **33**, 1166-1226.

[22] E. Gacz-Baitz, L. Radics, G.B. Ogenessian and V.A. Mnatsakanian (1978). Teucrins H1 – H4, novel clerodane-type diterpenes from *Teucrium hyrcanicum*, *Phytochemistry* **17**, 1967-1973.

[23] P.Y. Malakov, G.Y. Papanov and N.M. Mollov (1979). Furanoid diterpenes in the bitter fraction of *Teucrium polium* L., *Z. Naturforsch*. **34b**, 1570-1572.

[24] G. Savona, M. Paternostro and F. Piozzi (1979). New furanoid diterpenes from *Teucrium gnaphalodes* L'Her., *Tetrahedron Lett.* **4**, 379 – 382.

[25] T. Miyase, H. Kawasaki, T. Noro, A. Ueno, S. Fukushima and T. Takemoto (1981). Studies on the furanoid diterpenes from *Teucrium japonicum* Houtt, *Chem. Pharm. Bull.* **29**, 3561-3564.

[26] J. Fayos, F. Fernandez-Gadea, C. Pascaul, A. Perales, F. Piozzi, M. Rico, B. Rodriguez and G. Savona (1984). Correct structures of montanin C, teupolin I, and 12-*epi*-teucvin, three (12*R*)-Neoclerodan-20-12-olides isolated from the *Teucrium* species, *J. Org. Chem.* **49**, 1789-1793.

[27] G. Savona, F. Piozzi, M. Bruno, G. Dominguez, B. Rodriguez and O. Servettaz (1987). Teucretol, a *Neo*-Clerodane diterpenoid from *Teucrium creticum*, *Phytochemistry* **26**, 3285-3288.

[28] G. Savona, M. Bruno, F. Piozzi, O. Servettaz and B. Rodriguez (1984). *Neo*-Clerodane diterpenoids from *Teucrium massiliense*, *Phytochemistry* **23**, 849-852.

[29] D.E. Viney (1994). An Illustrated Flora of North Cyprus, Vol 1. Koeltz Scientific Books, Koenigstein, 697.

[30] J.E. El-Naggar and J. L. Beal (1984). Iridoids. A Review. *J. Nat. Prod.* **43**, 649-707.

[31] C.A. Boros and F.R. Stermitz (1990). Iridoids an Update Review, Part I. *J. Nat. Prod.* **53**, 1055-1147.

[32] C.A. Boros and F.R. Stermitz (1991). Iridoids an Update Review, Part II. *J. Nat. Prod.* **54**, 1173-1246.

[33] B. Dinda, S. Debnath and Y. Harigaya (2007). Naturally occurring iridoids, A Review, Part 1. *Chem. Pharm. Bull.* **55**(2), 159-222.

[34] B. Dinda, S. Debnath and Y. Harigaya (2007). Naturally occurring secoiridoids and bioactivity of naturally occurring iridoids and secoiridoids, A Review, Part 2. *Chem. Pharm. Bull.* **55**, 689-728.

[35] B. Dinda, D.R. Chowdhury and B.C. Chandra (2009). Naturally occurring iridoids, secoiridoids and their bioactivity, An updated review, part 3. *Chem. Pharm. Bull.* **57**, 765-796.

[36] E. Bedir, D. Tasdemir, İ. Çaliş, O. Zerbe and O. Sticher (1999). Neo-clerodane diterpenoids from *Teucrium polium*, *Phytochemistry* **51**, 921-925.

[37] E. Bedir, R. Manyam and I. A. Khan (2003). Neo-clerodane diterpenoids and phenylethanoid glycosides from *Teucrium chamaedrys* L., *Phytochemistry* **63**, 977-983.

[38] M. Elmastas, R. Erenler, B. Isnac, H. Aksit, O. Sen, N. Genc and I. Demirtas (2016). Isolation and identification of a new neo-clerodane diterpenoid from *Teucrium chamaedrys* L., *Nat. Prod. Res.* **30**, 299-304

[39] C. Jimenez and R. Riguera (1994). Phenylethanoid glycosides in plants: Structure and biological activity, *Nat. Prod. Rep.* **1994**, 591-606.

[40] Z. Xue and B. Yang (2016). Phenylethanoid glycosides: Research advances in their phytochemistry, pharmacological activity and pharmacokinetics, *Molecules* **21**, 991.

[41] J. Heilmann, İ. Çalış, H. Kırmızıbekmez, W. Schühly, Ş. Harput and O Sticher (2000). Radical scavenger activity of phenylethanoid glycosides in FMLP stimulated human polymorphonuclear leukocytes: Structure-activity relationships, *Planta Med.* **66**(8), 746-748.

[42] S.D. Marino, C. Festa, F. Zollo, F. Incollingo, G. Raimo, G. Evangelista and M. Iorizzi (2012). Antioxidant activity of phenolic and phenylethanoid glycosides from *Teucrium polium* L., *Food Chem.* **133**, 21-28.

[43] Y. Dai, G. Han, S. Xu, Y. Yuan, C. Zhao and T. Ma (2020). Echinacoside suppresses amyloidogenesis and modulates F-actin remodeling by targeting the ER stress sensor PERK in a mouse model of alzheimer's disease, *Frontiers in Cell and Developmental Biology* **8**, 1-20.

[44] J.B. Harborne (1966). Caffeic acid ester distribution in higher plants, *Z. Naturforsch*. **21b**, 604-605.

[45] J.A. Pedersen (2000). Distribution and taxonomic implications of some phenolics in the family Lamiaceae determined by ESR spectroscopy, Biochemical Systematics and Ecology **28**, 229-253.

[46] J.P. Alvarez , F Sáez-Royuela, E.G. Peña, A.L. Morante, A.V. Osés and J.M. Lorente (2001). Acute hepatitis due to ingestion of *Teucrium chamaedrys* infusions, *Gastroenterol. Hepatol.* **24**, 240-243.

[47] D. Polymeros, D. Kamberoglou and V. Tzias (2002). Acute cholestatic hepatitis caused by *Teucrium polium* (golden germander) with transient appearance of antimitochondrial antibody, *J. Clin. Gastroenterol.* **34**, 100-101.

[48] R. Gagliano Candela, S. Rosselli, M. Bruno and G. Fontana (2020). A Review of the phytochemistry, traditional uses and biological activities of the essential oils of genus *Teucrium*, *Planta Med.* DOI 10.1055/a-1293-5768

[49] M.-E. Grafakou, C. Barda and H. Skaltsa (2020). Secondary metabolites of *Teucrium* species with toxic effects. In: *Teucrium* species: Biology and applications, Ed. Milan Stanković, Springer, pp 211-230.

[50] J.B. Harborne, F.A. Thomás Barberán, C. A. Williams and M. I. Gil (1986). A chemotaxonomic study of flavonoids from european *Teucrium* species, *Phytochemistry* **25**, 2811-2816.

[51] A. Ulubelen, G. Topçu and U. Kolak (2005). Labiatae flavonoids and their bioactivity. In: studies in Natural Products Chemistry, *ed*: Atta-ur Rahman, Elsevier Science, Amsterdam, Netherlands, Vol. 30, pp 233-302.

[52] G. Valentini, B. Bellomaria and N. Arnold (1997). Essential oil of *Teucrium creticum* L. from Cyprus, *J. Essent.Oil Res*. **9**: 649-652.

[53] M. Al-Masri, G. Omar, A. Taha, A. Abu Alsoud, E. Tawafsha, R. Basheer, M. Al-Akhras and R. Taradeh (2019). Antimicrobial activities of *Teucrium creticum* against reference microbial strains and multi-drug resistant bacteria isolated at an oncology, *J. Advan. Microbiol*. **17**, 1-7.

A C G
publications
© 2021 ACG Publications

Supporting Information

***Rec. Nat. Prod.* 15:6 (2021) 487-502**

Secondary Metabolites from *Teucrium creticum* L.

Azmi Hanoğlu[1], Duygu Yiğit Hanoğlu[2], Nilay Demirel[1], Hasan Soliman Yusufoğlu[3] and İhsan Çalış[1]*

[1]Near East University,Faculty of Pharmacy, Department of Pharmacognosy, Lefkoşa, TRNC

[2]Near East University,Faculty of Pharmacy, Department of Pharmaceutical Botany, Lefkoşa, TRNC

[3]Prince Sattam Bin Abdulaziz University, Department of Pharmacognosy, Al-Kharj–11942, Saudi Arabia

Table of Contents	Page
Figure S1: ^{1}H-NMR Spectrum of 8-*O*-Acetylharpagide (**1**) (400 MHz, CD_3OD)	3
Figure S2: ^{13}C-NMR Spectrum of 8-*O*-Acetylharpagide (**1**) (100 MHz, CD_3OD)	3
Figure S3: ^{1}H-NMR Spectrum of Teuhircoside (**2**) (400 MHz, CD_3OD)	4
Figure S4: ^{13}C-NMR Spectrum of Teuhircoside (**2**) (100 MHz, CD_3OD)	4
Figure S5: ^{1}H-NMR Spectrum of Verbascoside (= Acteoside) (**3**) (400 MHz, CD_3OD)	5
Figure S6: ^{13}C-NMR Spectrum of Verbascoside (= Acteoside) (**3**) (100 MHz, CD_3OD)	5
Figure S7: ^{1}H-NMR Spectrum of Lavandulifolioside (**5**) (400 MHz, CD_3OD)	6
Figure S8: ^{13}C-NMR Spectrum of Lavandulifolioside (**5**) (100 MHz, CD_3OD)	6
Figure S9: Positive ion HRMS of Teucrin H3 (= 19-acetylgnaphalin) (**5**)	7
Figure S10: ^{1}H-NMR Spectrum of Teucrin H3 (= 19-acetylgnaphalin) (**5**) (500 MHz, CD_3OD)	7
Figure S11: ^{13}C-NMR Spectrum of Teucrin H3 (= 19-acetylgnaphalin) (**5**) (125 MHz, CD_3OD)	8
Figure S12: COSY of Teucrin H3 (= 19-acetylgnaphalin) (**5**)	9
Figure S13: HSQC of Teucrin H3 (= 19-acetylgnaphalin) (**5**)	9
Figure S14: HSQC of Teucrin H3 (= 19-acetylgnaphalin) (**5**) (f1: δ 30 – 75; f2: δ 5.5 – 1.6)	10
Figure S15: HSQC of Teucrin H3 (= 19-acetylgnaphalin) (**5**) (f1: δ 14 – 34; f2: δ 2.7 – 0.8)	10
Figure S16: HMBC of Teucrin H3 (= 19-acetylgnaphalin) (**5**)	11
Figure S17: NOESY of Teucrin H3 (= 19-acetylgnaphalin) (**5**)	12

Figure S18: Positive ion HRMS of Teucjaponin B (**6**)	13
Figure S19: ^{1}H-NMR Spectrum of Teucjaponin B (**6**) (500 MHz, CD_3OD)	13
Figure S20:^{13}C-NMR Spectrum (125 MHz, CD_3OD) and DEPT-135 of Teucjaponin B (**6**)	14
Figure S21: COSY of Teucjaponin B (**6**)	15
Figure S22: HSQC of Teucjaponin B (**6**)	15
Figure S23: HSQC of Teucjaponin B (**6**) (f1: δ 15 – 55; f2: δ 2.6 – 0.7)	16
Figure S24: HMBC of Teucjaponin B (**6**)	16
Figure S25: HMBC of Teucjaponin B (**6**) (f1: δ 15 – 75; f2: δ 5.2 – 0.6)	17
Figure S26: NOESY of Teucjaponin B (**6**)	17
Figure S27: Positive ion HRMS of Teucretol (**7**)	18
Figure S28: ^{1}H-NMR Spectrum of Teucretol (**7**) (500 MHz, CD_3OD)	18
Figure S29: ^{13}C-NMR Spectrum (125 MHz, CD_3OD) and DEPT-135 of Teucretol (**7**)	19
Figure S30: COSY of Teucretol (**7**)	20
Figure S31: HSQC of Teucretol (**7**)	20
Figure S32: HSQC of Teucretol (**7**) (f1: δ 15 – 55; f2: δ 2.4 – 0.8)	21
Figure S33: HMBC of Teucretol (**7**)	21
Figure S34: NOESY of Teucretol (**7**)	22
Figure S35: Positive ion HRMS of Diacetylteumassilin (**8**)	23
Figure S36. ^{1}H-NMR Spectrum of Diacetylteumassilin (**8**) (500 MHz, CD_3OD)	23
Figure S37: ^{13}C-NMR Spectrum (125 MHz, CD_3OD) and DEPT-135 of Diacetylteumassilin (**8**)	24
Figure S38: COSY of Diacetylteumassilin (**8**)	25
Figure S39: HSQC of Diacetylteumassilin (**8**)	25
Figure S40: HSQC of Diacetylteumassilin (**8**) (f1: δ 15 – 50; f2: δ 3.1 – 0.6)	26
Figure S41: HMBC of Diacetylteumassilin (**8**)	26
Figure S42: NOESY of Diacetylteumassilin (**8**)	27

© 2021 ACG Publications. All rights reserved.

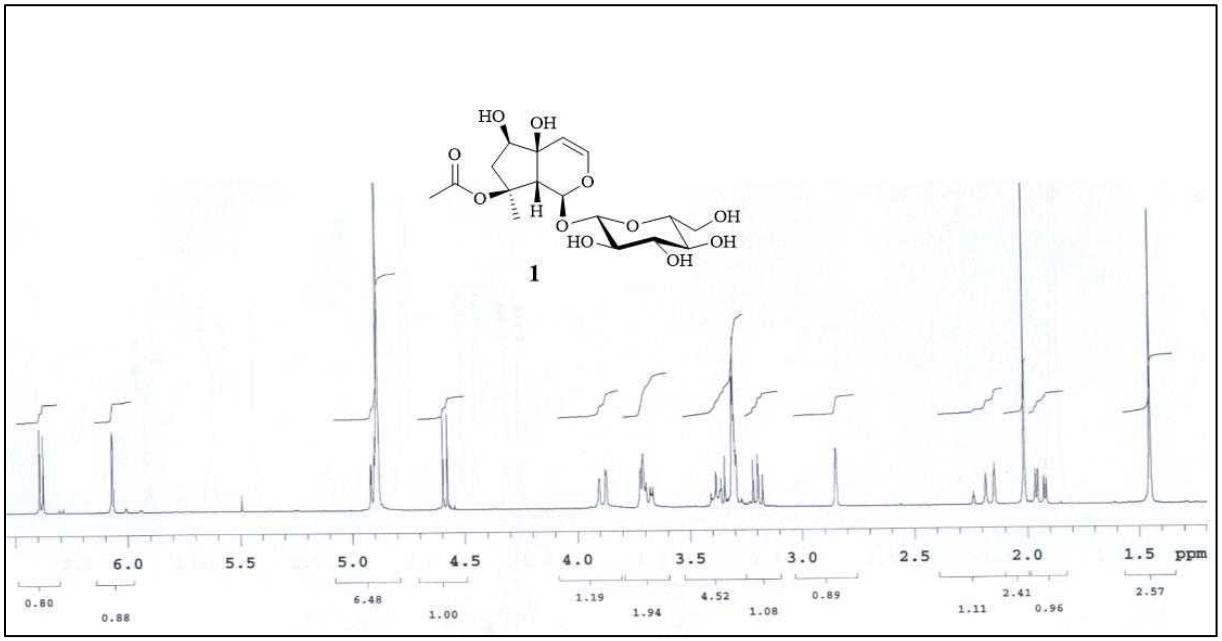

Figure S1: ^{1}H-NMR Spectrum of 8-*O*-Acetylharpagide (**1**) (400 MHz, CD_3OD)

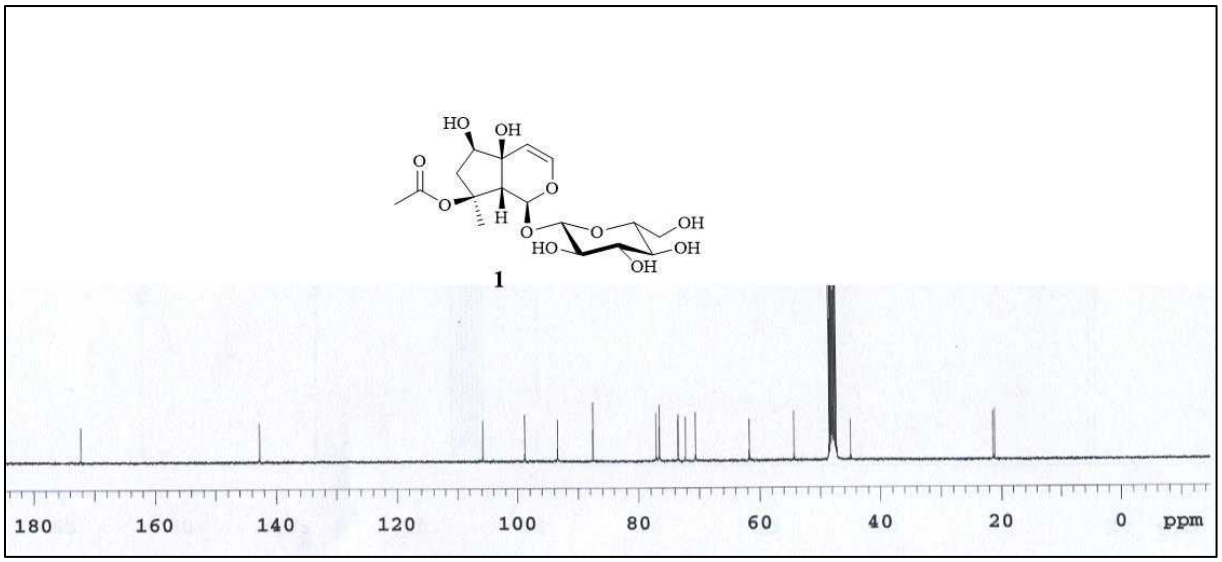

Figure S2: ^{13}C-NMR Spectrum of 8-*O*-Acetylharpagide (**1**) (100 MHz, CD_3OD)

© 2021 ACG Publications. All rights reserved.

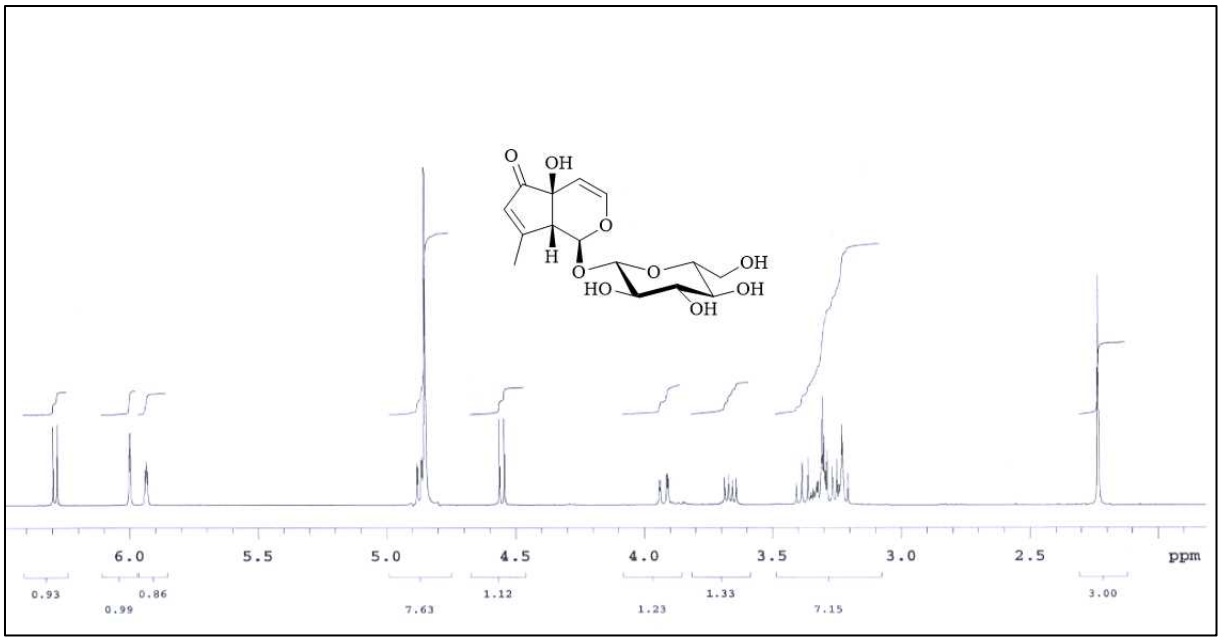

Figure S3: ^{1}H-NMR Spectrum of Teuhircoside (**2**) (400 MHz, CD_3OD)

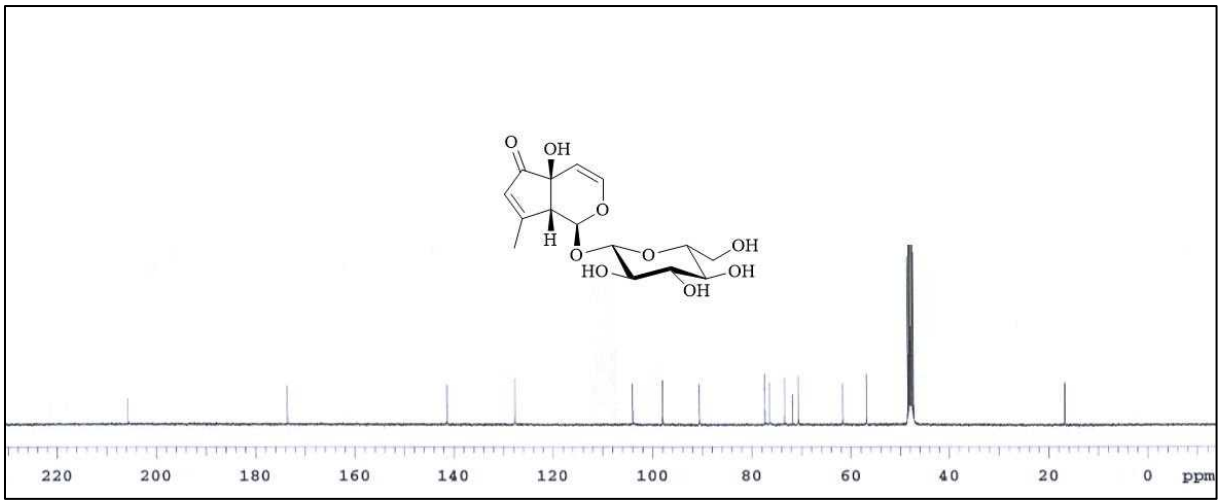

Figure S4: ^{13}C-NMR Spectrum of Teuhircoside (**2**) (100 MHz, CD_3OD)

© 2021 ACG Publications. All rights reserved.

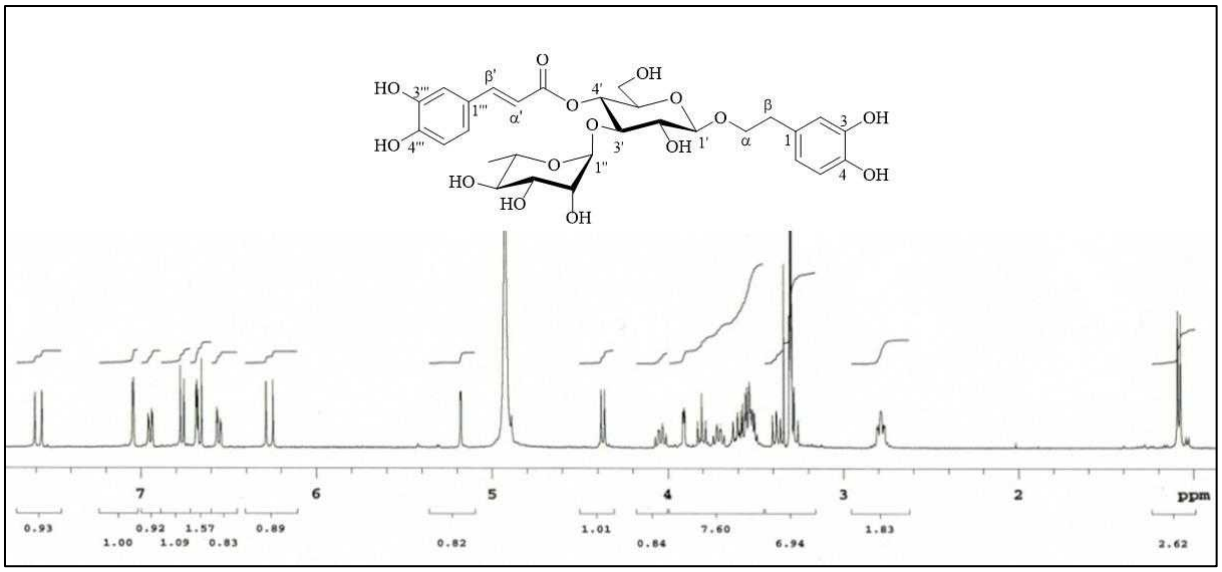

Figure S5: ^{1}H-NMR Spectrum of Verbascoside (= Acteoside) (**3**) (400 MHz, CD_3OD)

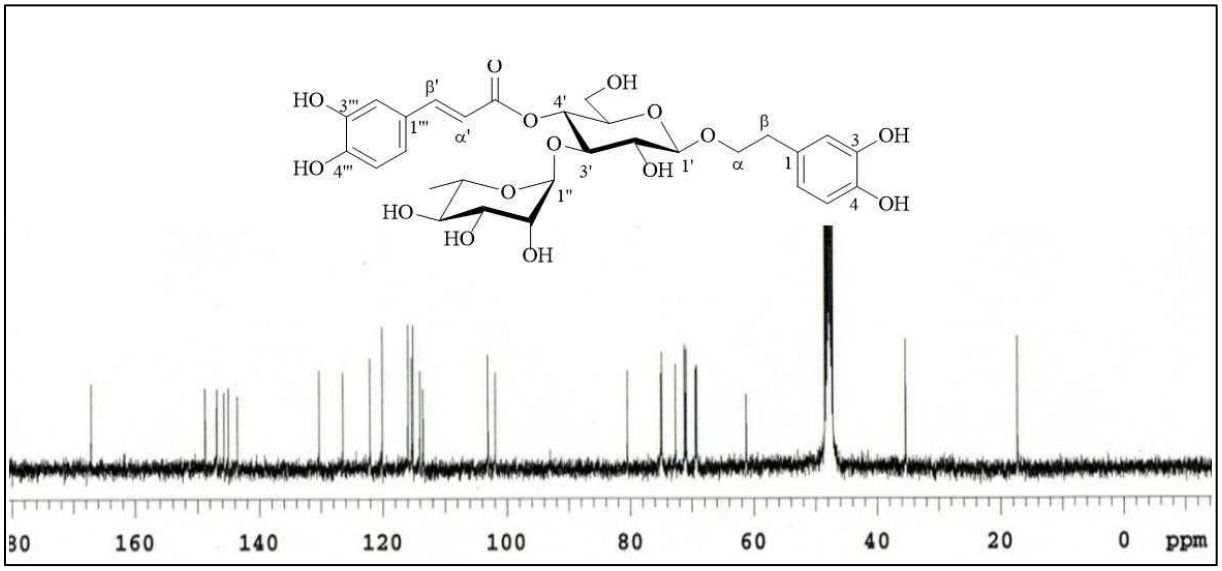

Figure S6: ^{13}C-NMR Spectrum of Verbascoside (= Acteoside) (**3**) (100 MHz, CD_3OD)

© 2021 ACG Publications. All rights reserved.

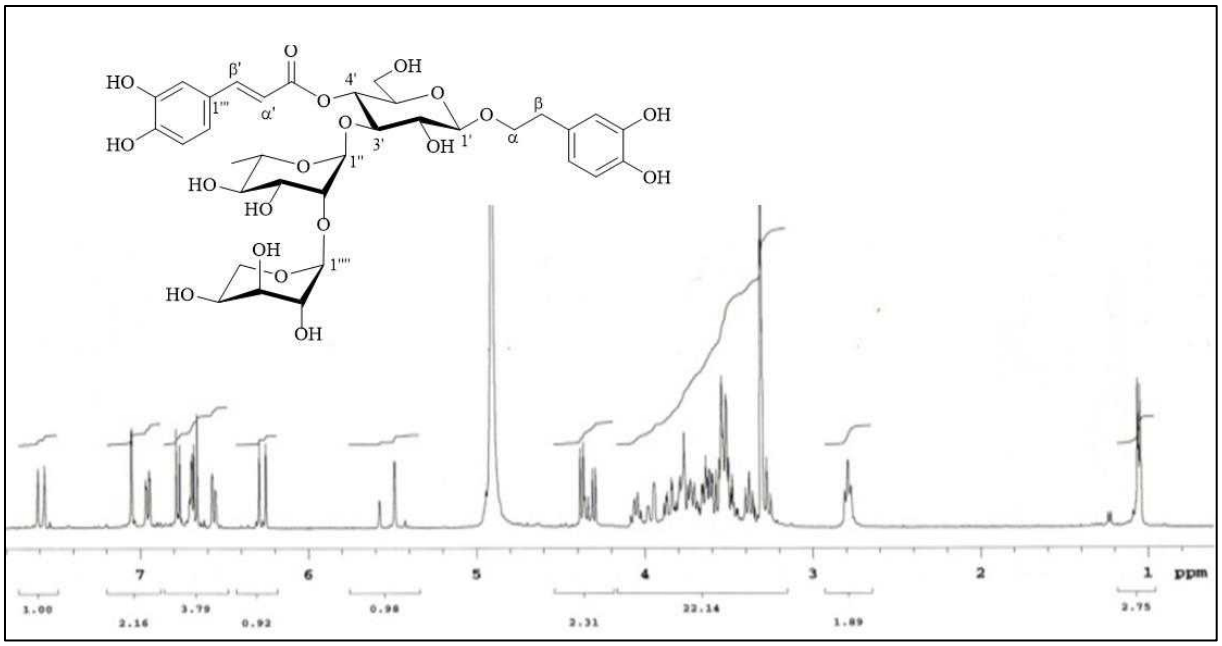

Figure S7: ^{1}H-NMR Spectrum of Lavandulifolioside (**5**) (400 MHz, CD_3OD)

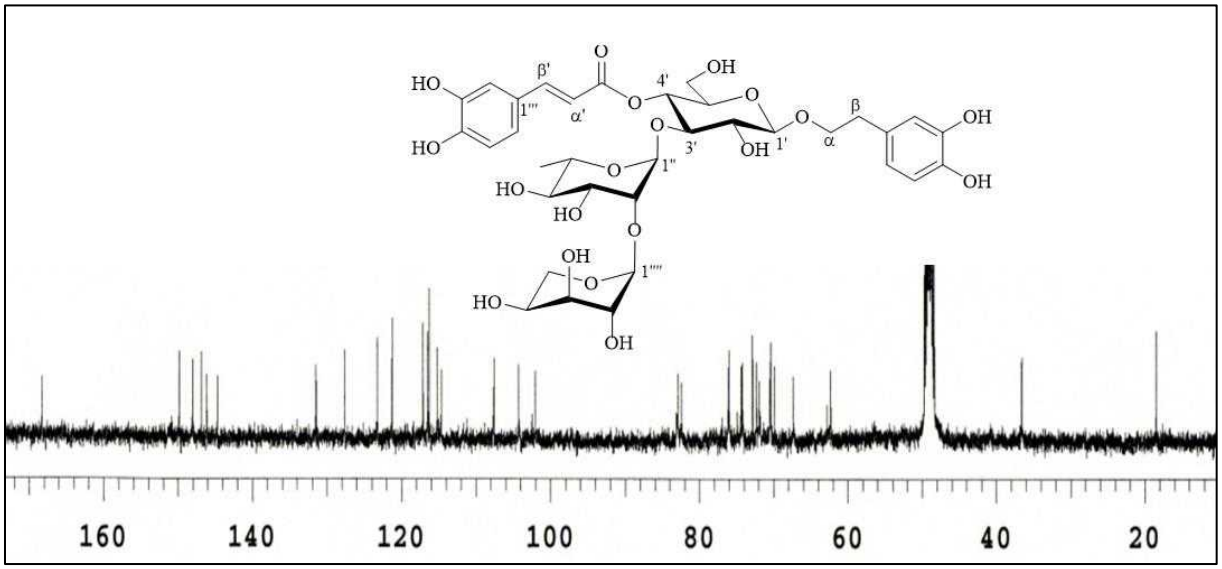

Figure S8: ^{13}C-NMR Spectrum of Lavandulifolioside (**5**) (100 MHz, CD_3OD)

© 2021 ACG Publications. All rights reserved.

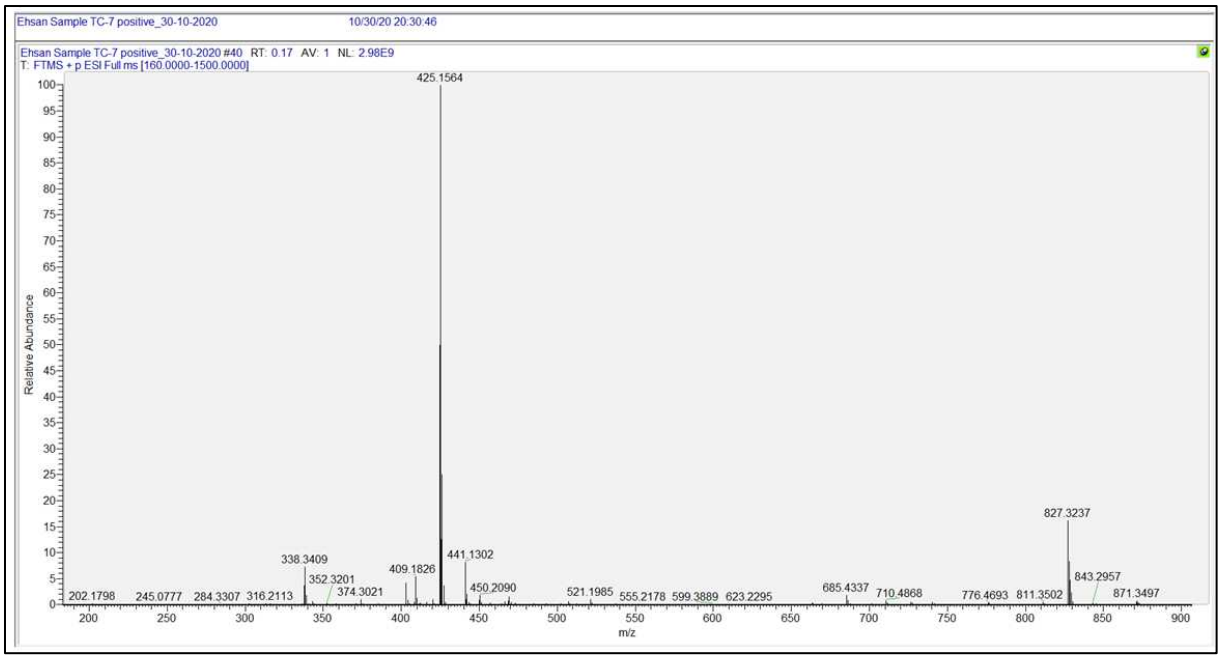

Figure S9: Positive ion HRMS of Teucrin H3 (= 19-acetylgnaphalin) (**5**)

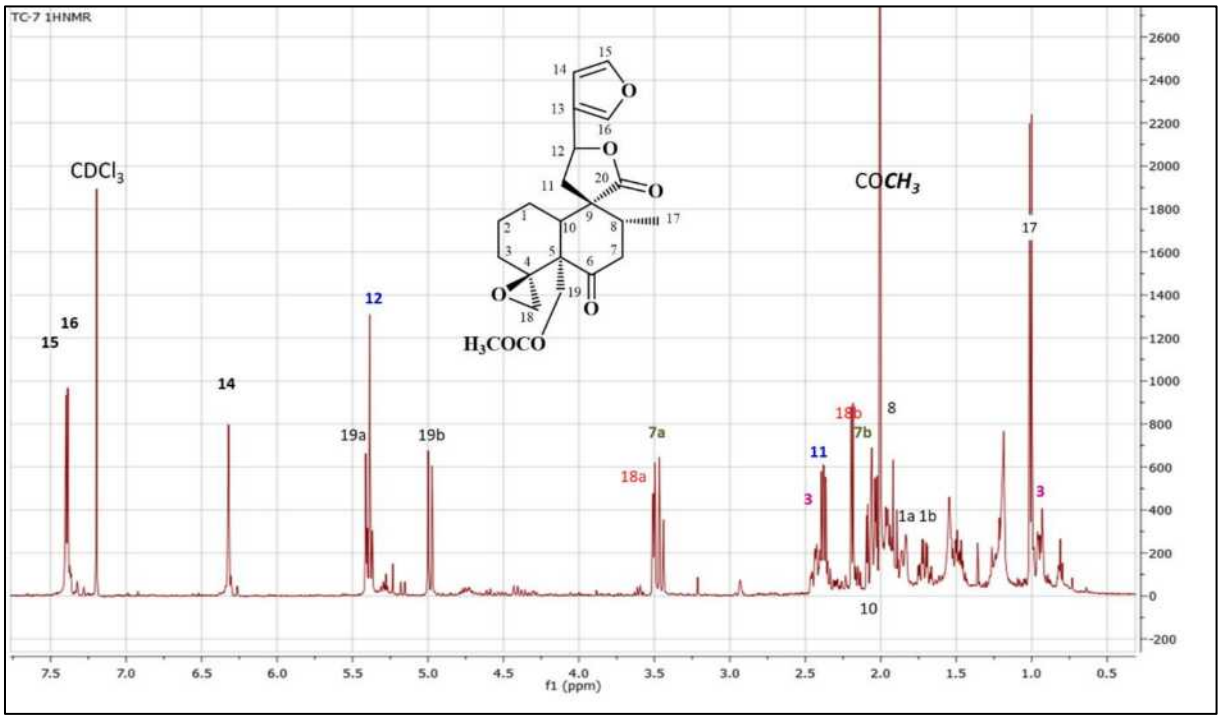

Figure S10: ^{1}H-NMR Spectrum of Teucrin H3 (= 19-acetylgnaphalin) (**5**) (500 MHz, CD_3OD)

© 2021 ACG Publications. All rights reserved.

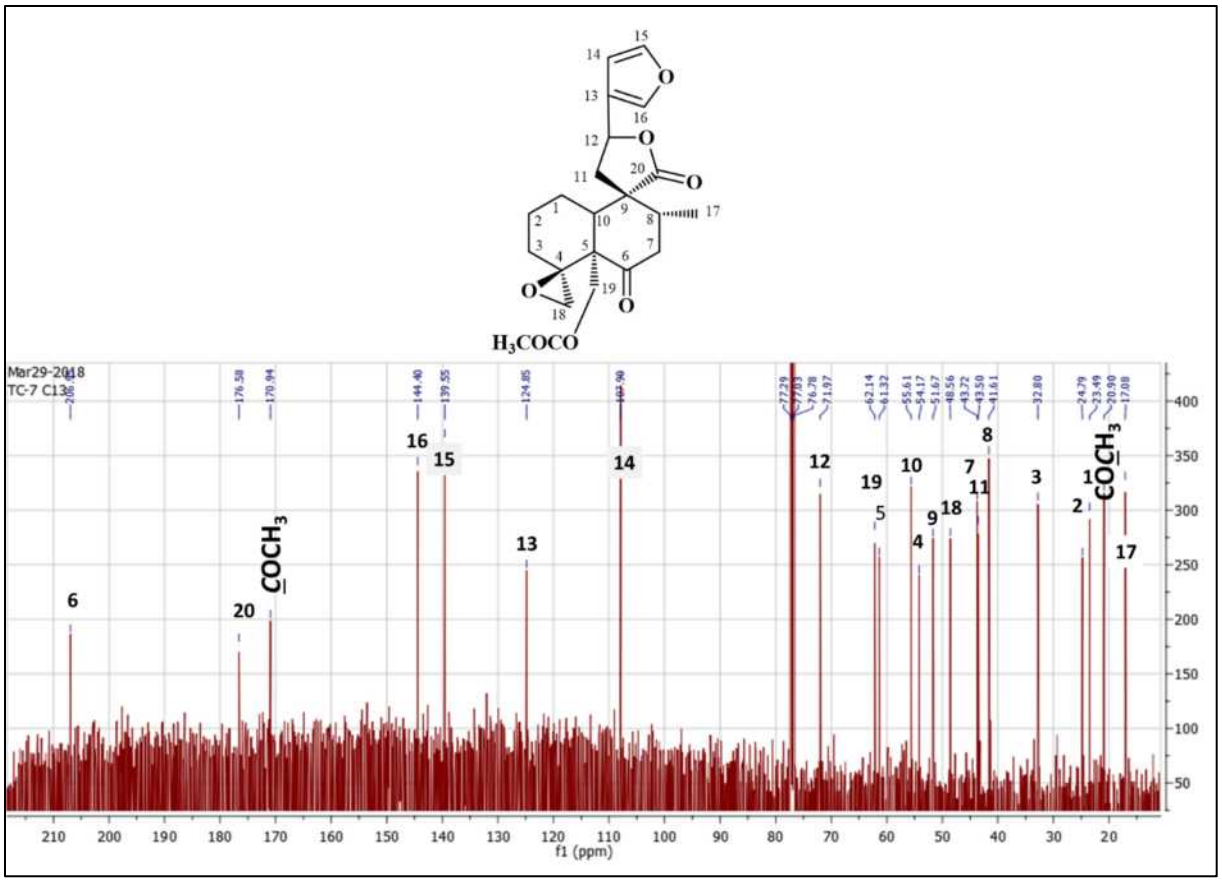

Figure S11: ^{13}C-NMR Spectrum of Teucrin H3 (= 19-acetylgnaphalin) (**5**) (125 MHz, CD_3OD)

© 2021 ACG Publications. All rights reserved.

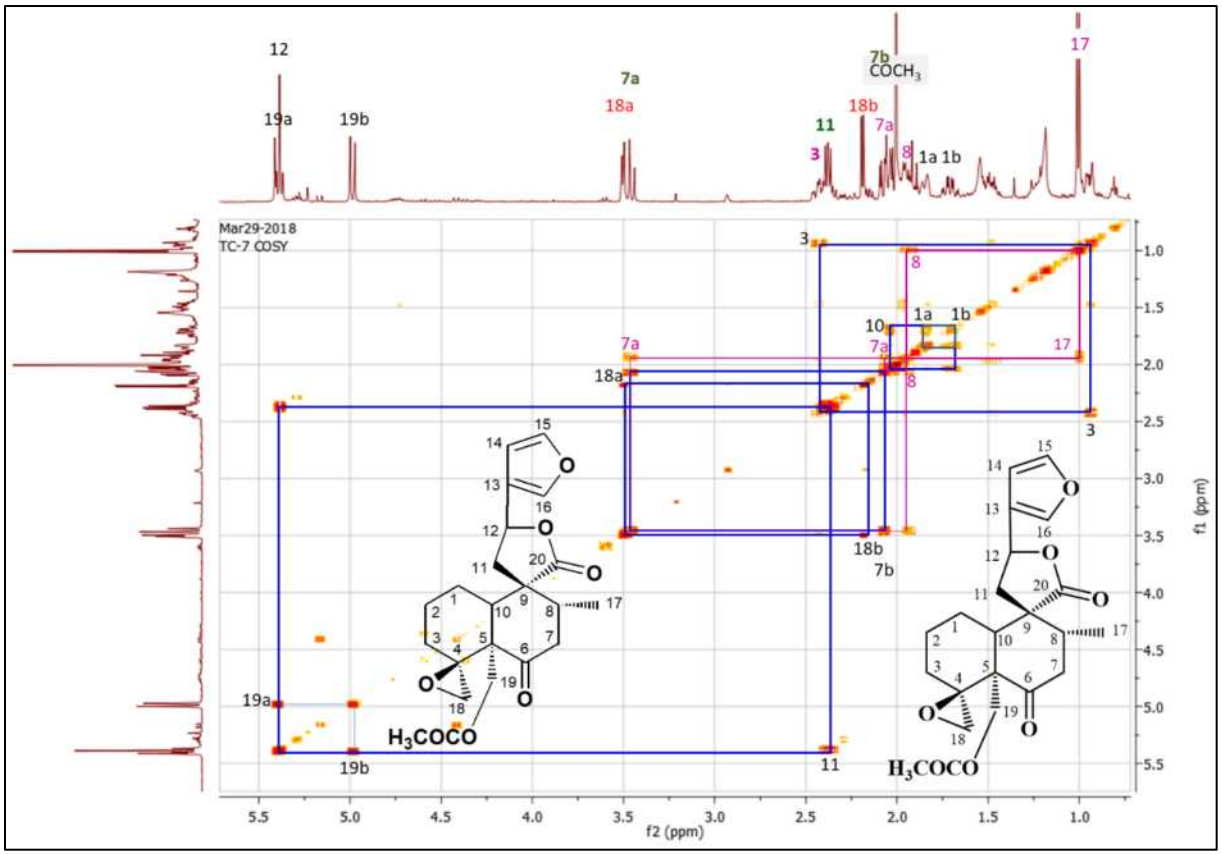

Figure S12: COSY of Teucrin H3 (= 19-acetylgnaphalin) (**5**)

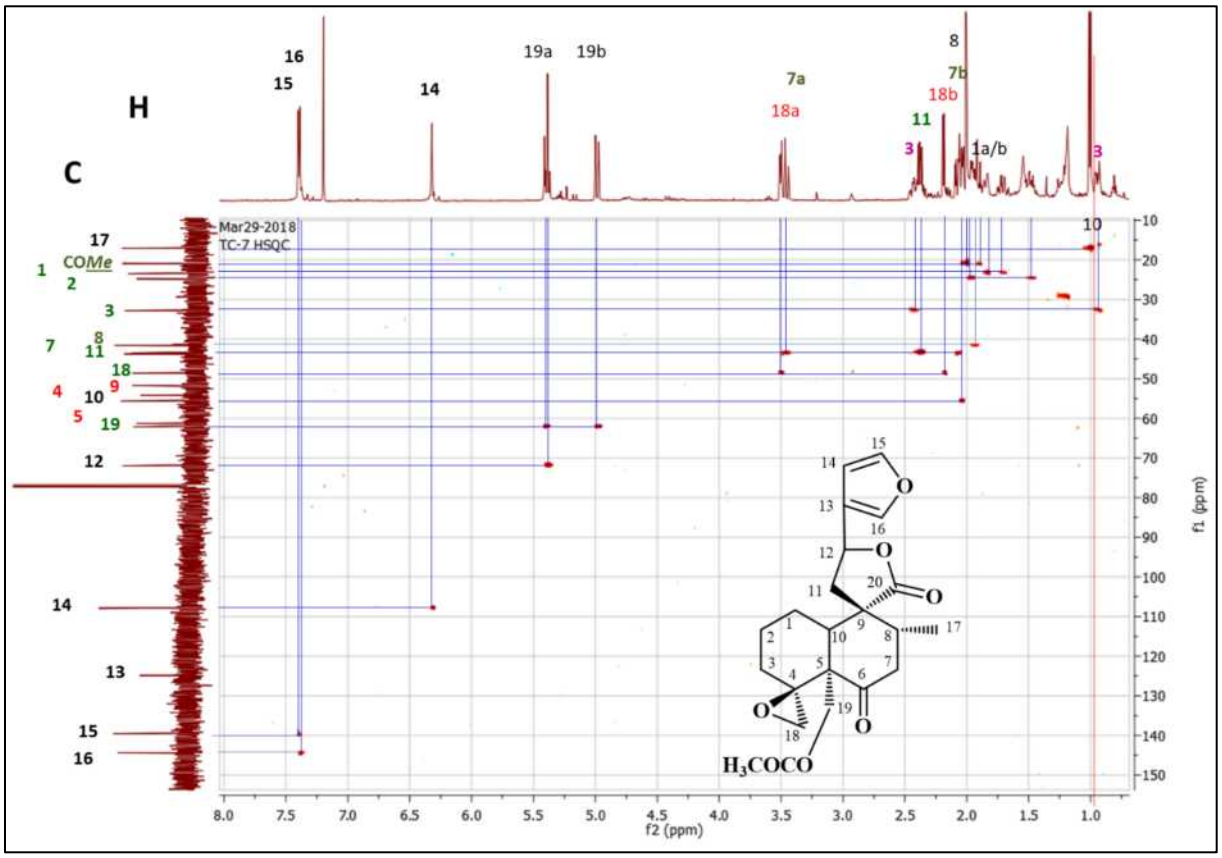

Figure S13: HSQC of Teucrin H3 (= 19-acetylgnaphalin) (**5**)

© 2021 ACG Publications. All rights reserved.

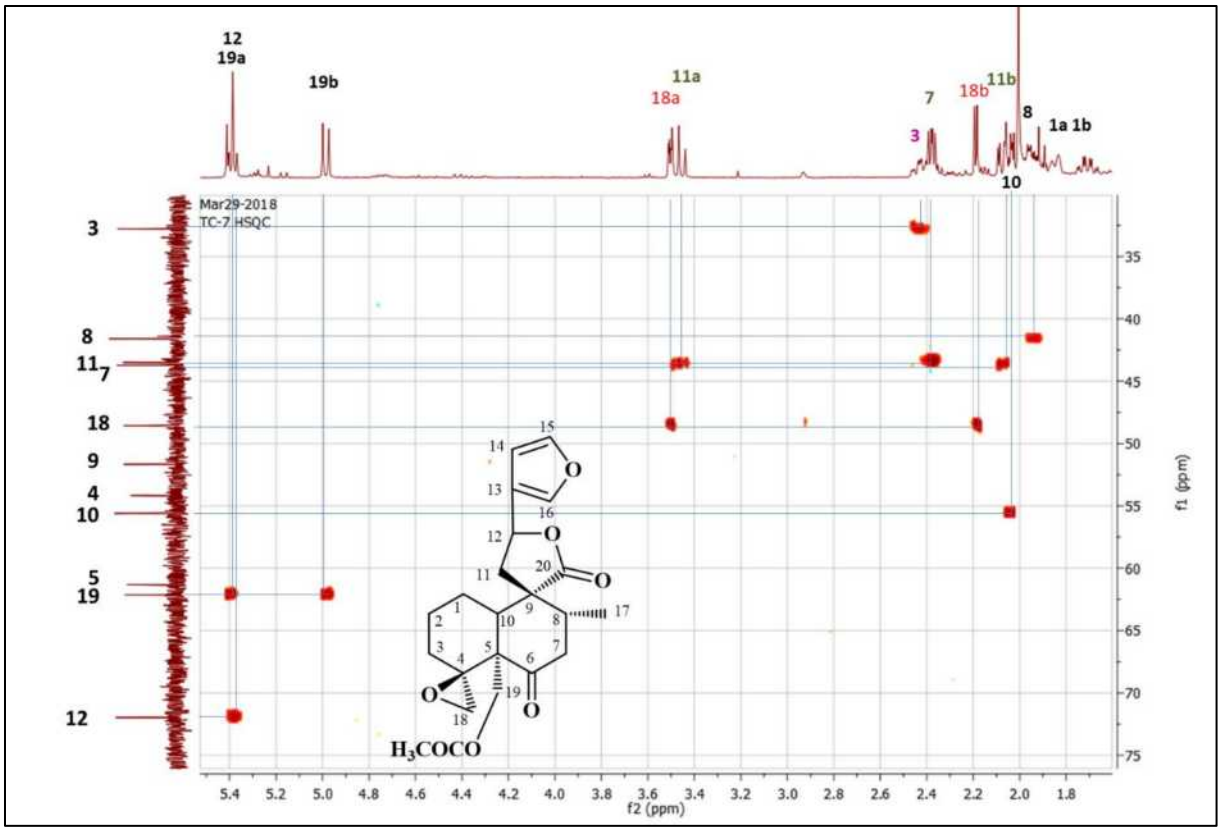

Figure S14:HSQC of Teucrin H3 (= 19-acetylgnaphalin) (**5**) (f1: δ 30 – 75; f2: δ 5.5 – 1.6)

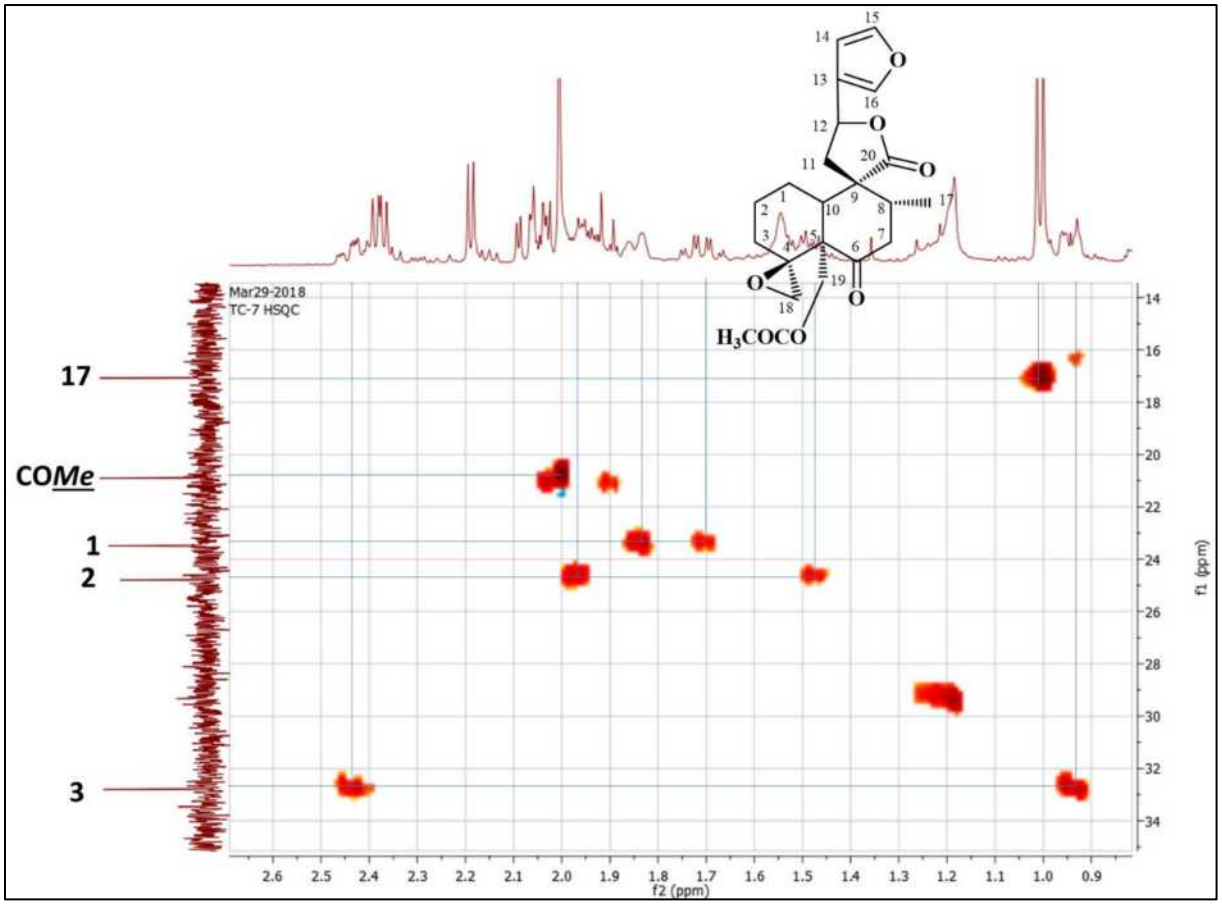

Figure S15: HSQC of Teucrin H3 (= 19-acetylgnaphalin) (**5**) (f1: δ 14 – 34; f2: δ 2.7 – 0.8)

© 2021 ACG Publications. All rights reserved.

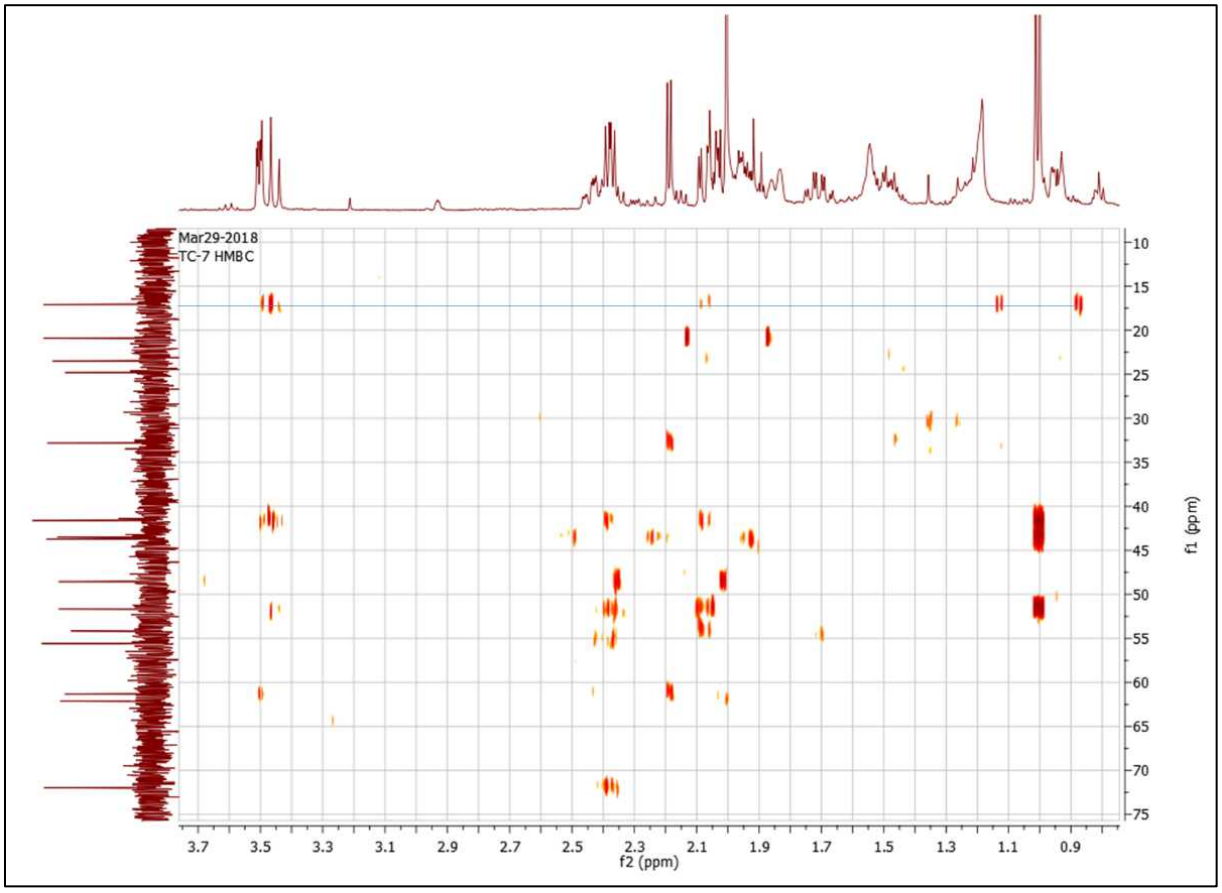

Figure S16: HMBC of Teucrin H3 (= 19-acetylgnaphalin) (**5**)

© 2021 ACG Publications. All rights reserved.

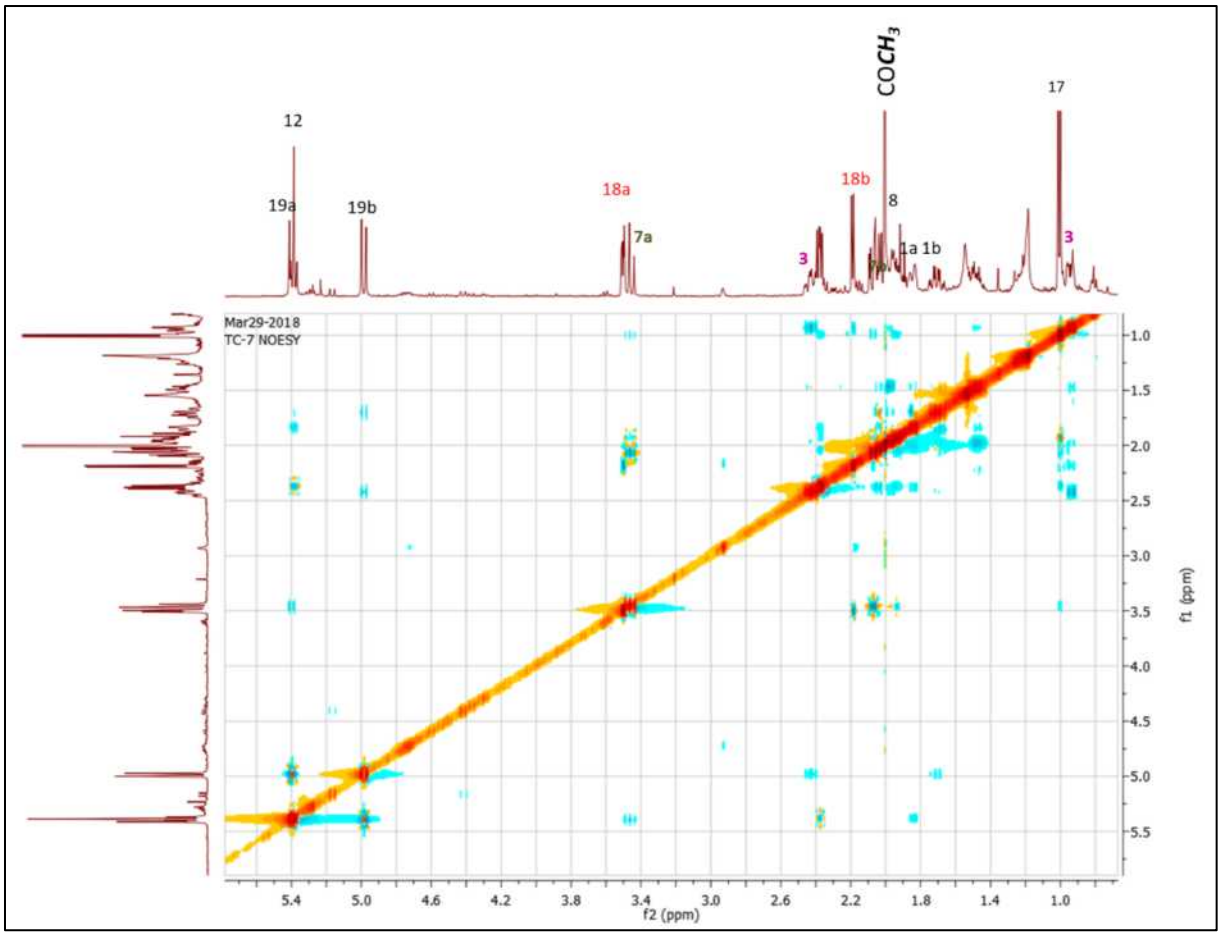

Figure S17: NOESY of Teucrin H3 (= 19-acetylgnaphalin) (**5**)

© 2021 ACG Publications. All rights reserved.

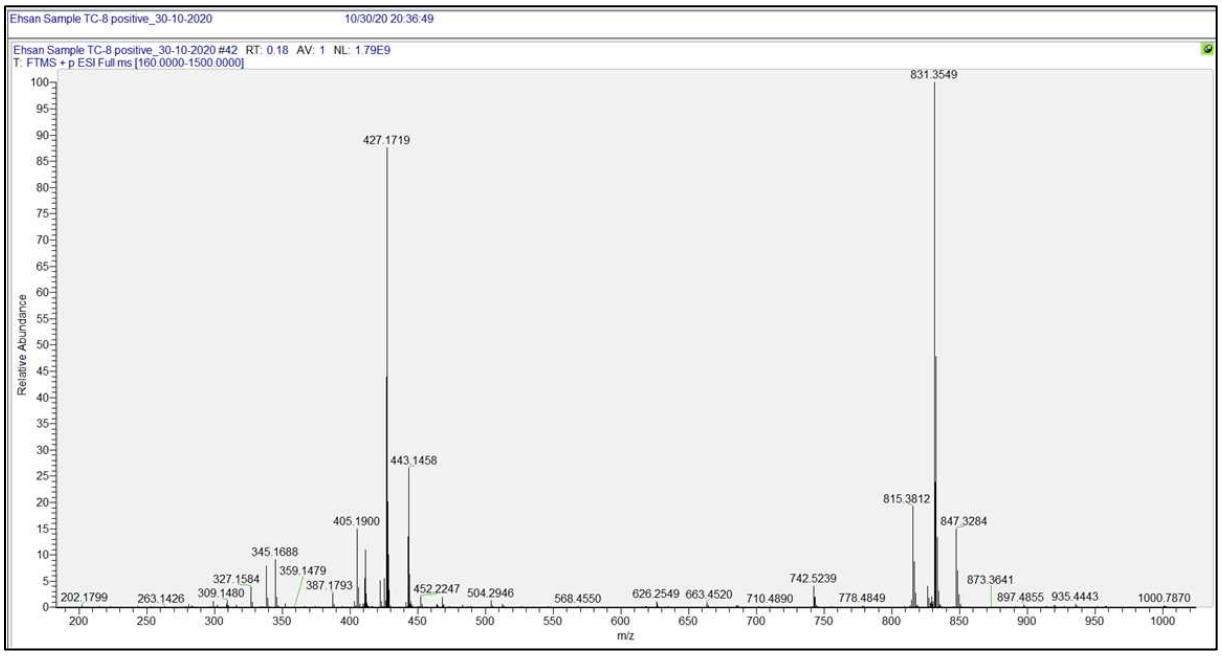

Figure S18: Positive ion HRMS of Teucjaponin B (**6**)

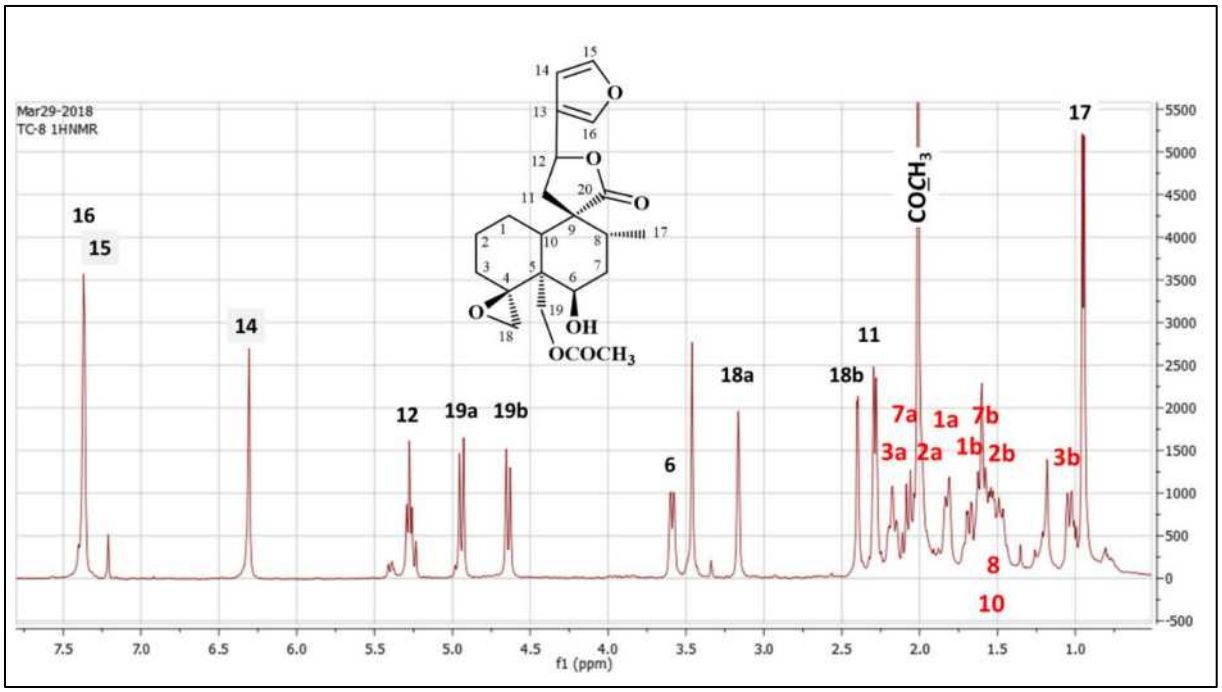

Figure S19: ^{1}H-NMR Spectrum of Teucjaponin B (**6**)(500 MHz, CD_3OD)

© 2021 ACG Publications. All rights reserved.

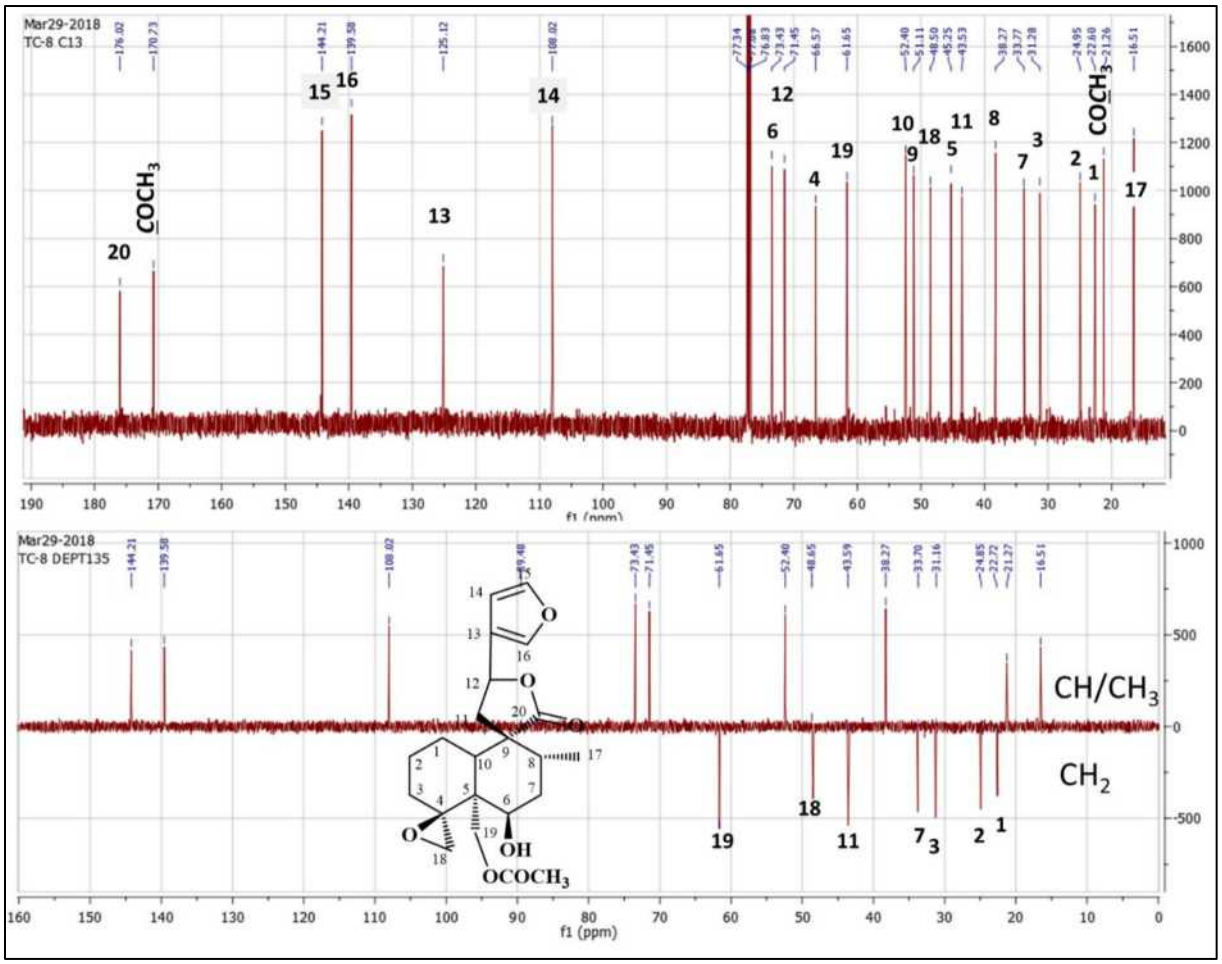

Figure S20: ^{13}C-NMR Spectrum (125 MHz, CD_3OD) and DEPT-135 of Teucjaponin B (**6**)

© 2021 ACG Publications. All rights reserved.

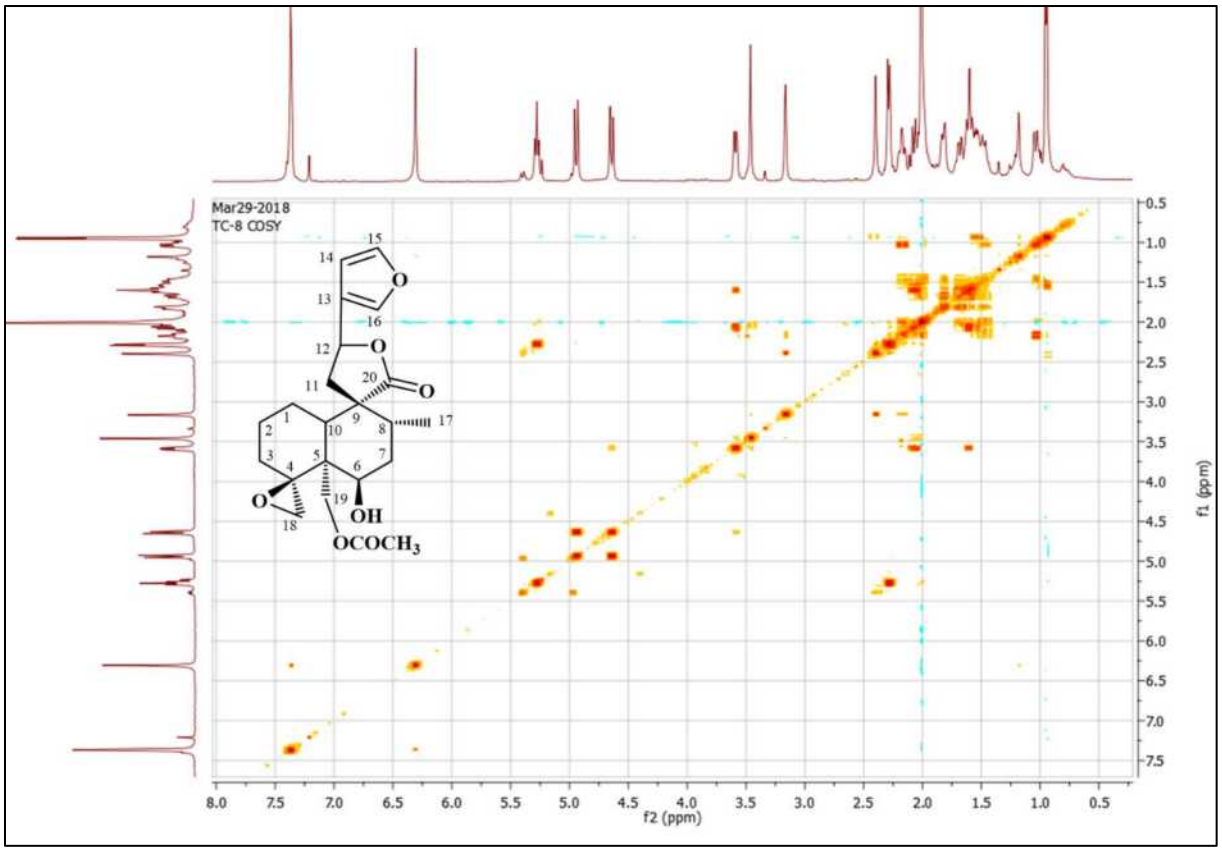

Figure S21: COSY of Teucjaponin B (**6**)

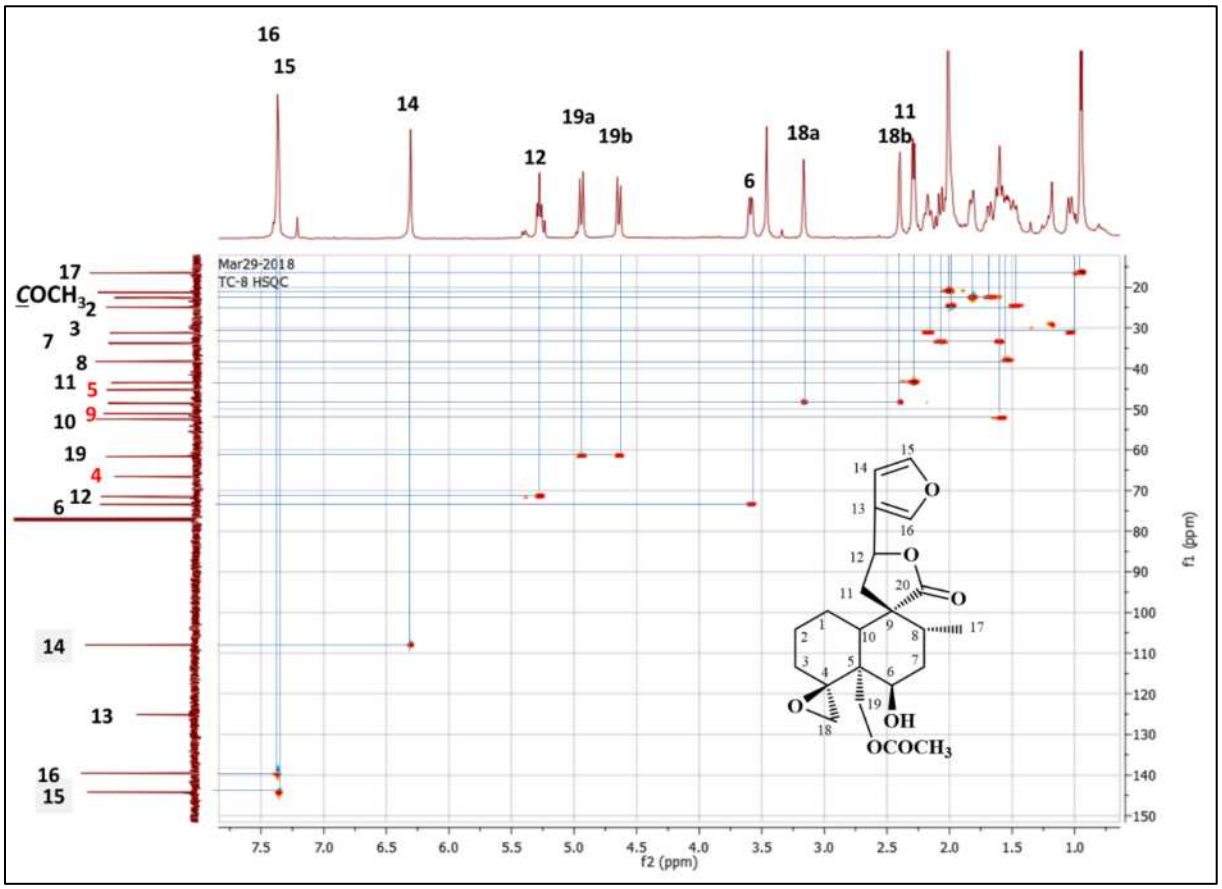

Figure S22: HSQC of Teucjaponin B (**6**)

© 2021 ACG Publications. All rights reserved.

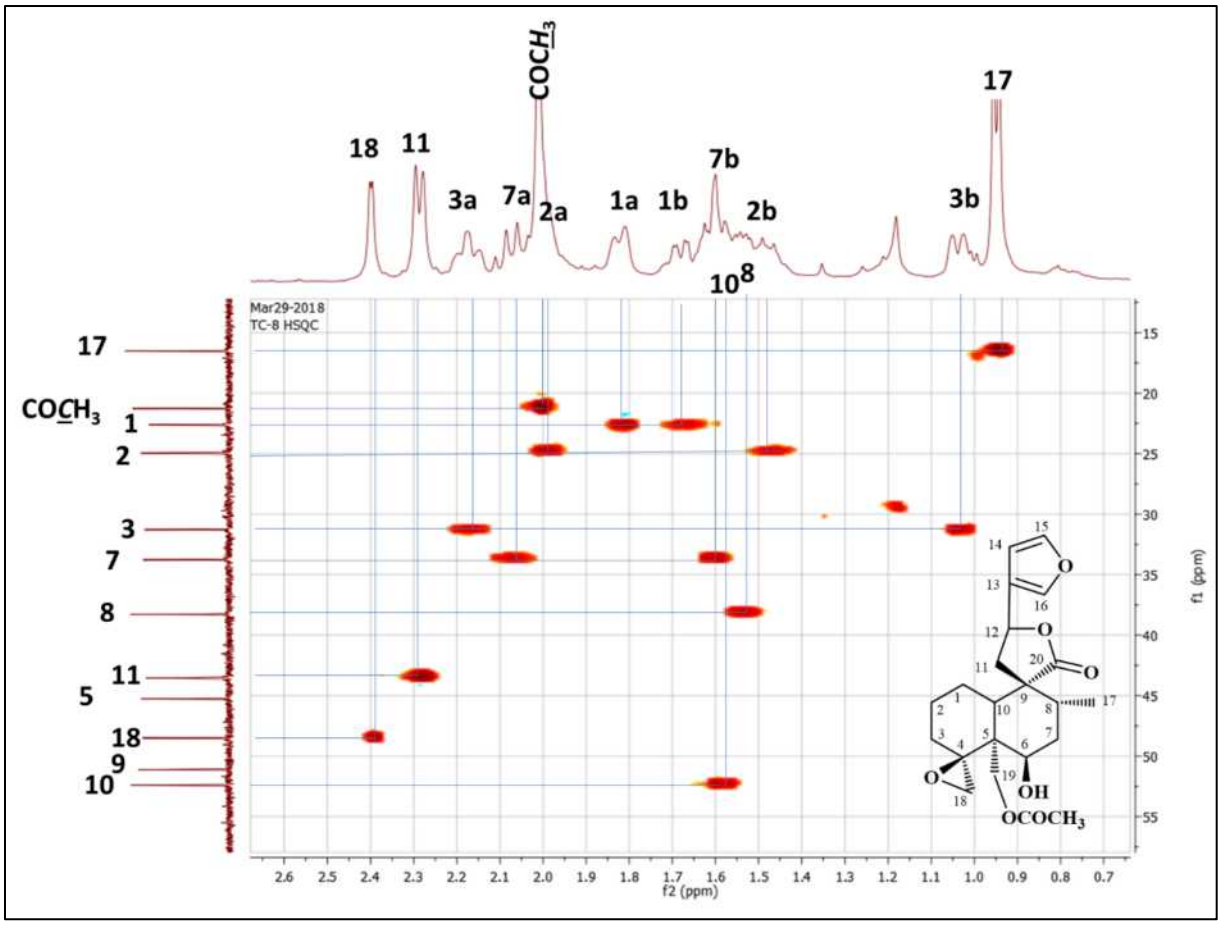

Figure S23: HSQC of Teucjaponin B (**6**)(f1: δ 15 – 55; f2: δ 2.6 – 0.7)

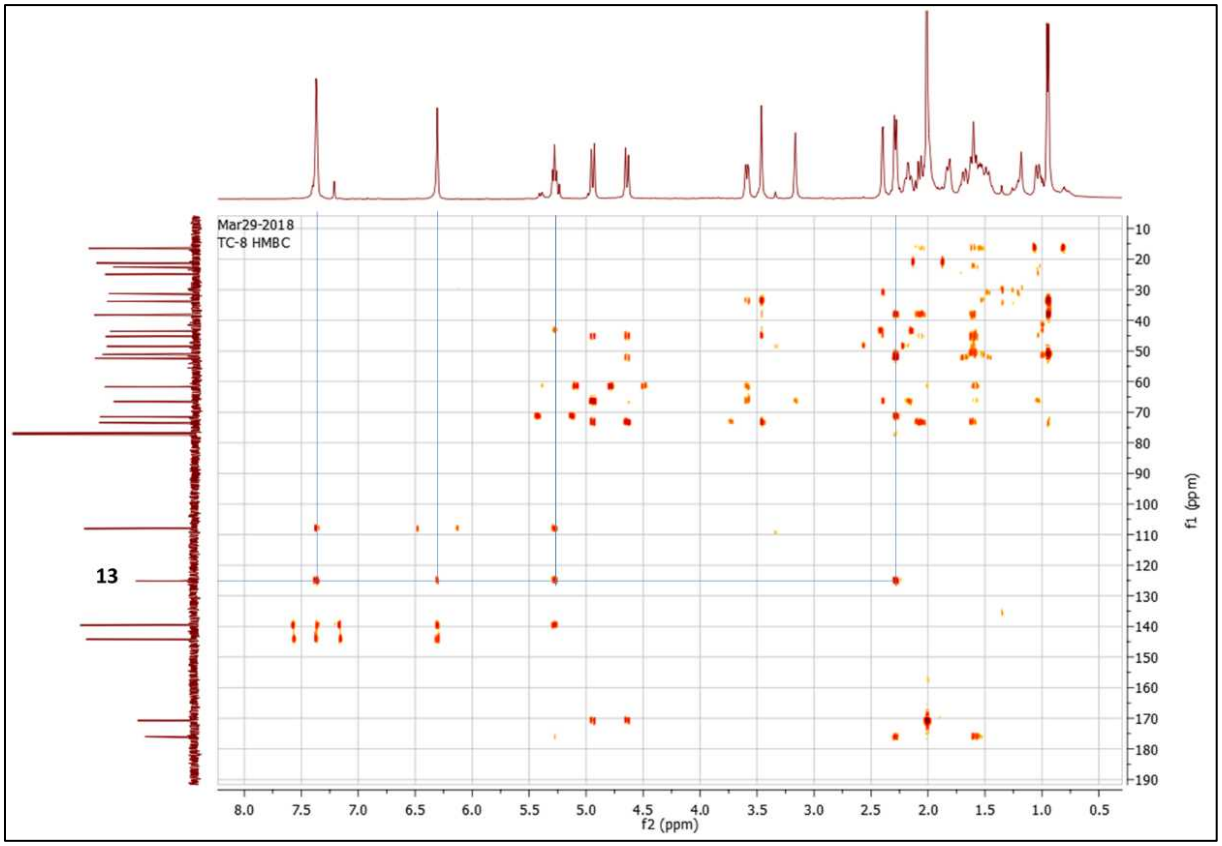

Figure S24: HMBC of Teucjaponin B (**6**)

© 2021 ACG Publications. All rights reserved.

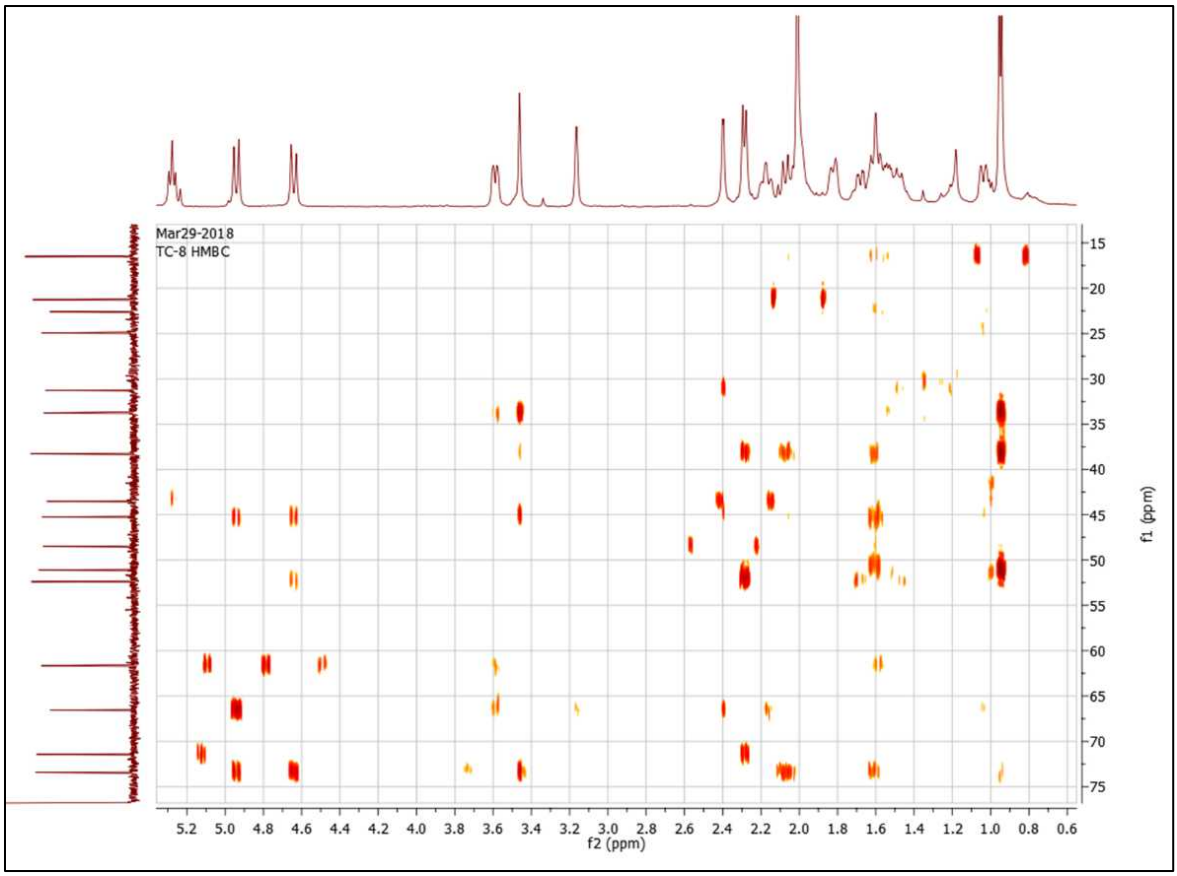

Figure S25: HMBC of Teucjaponin B (**6**)(f1: δ 15 – 75; f2: δ5.2 – 0.6)

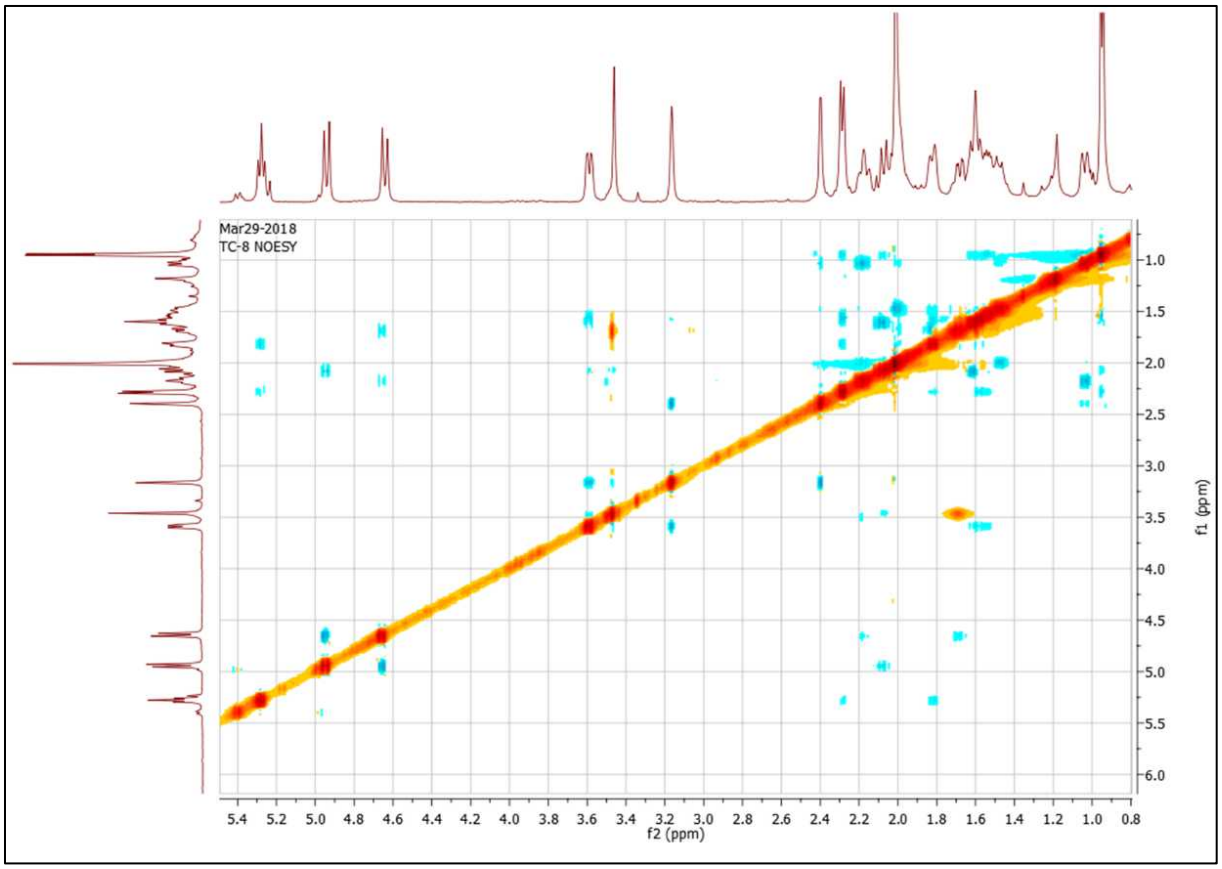

Figure S26: NOESY of Teucjaponin B (**6**)

© 2021 ACG Publications. All rights reserved.

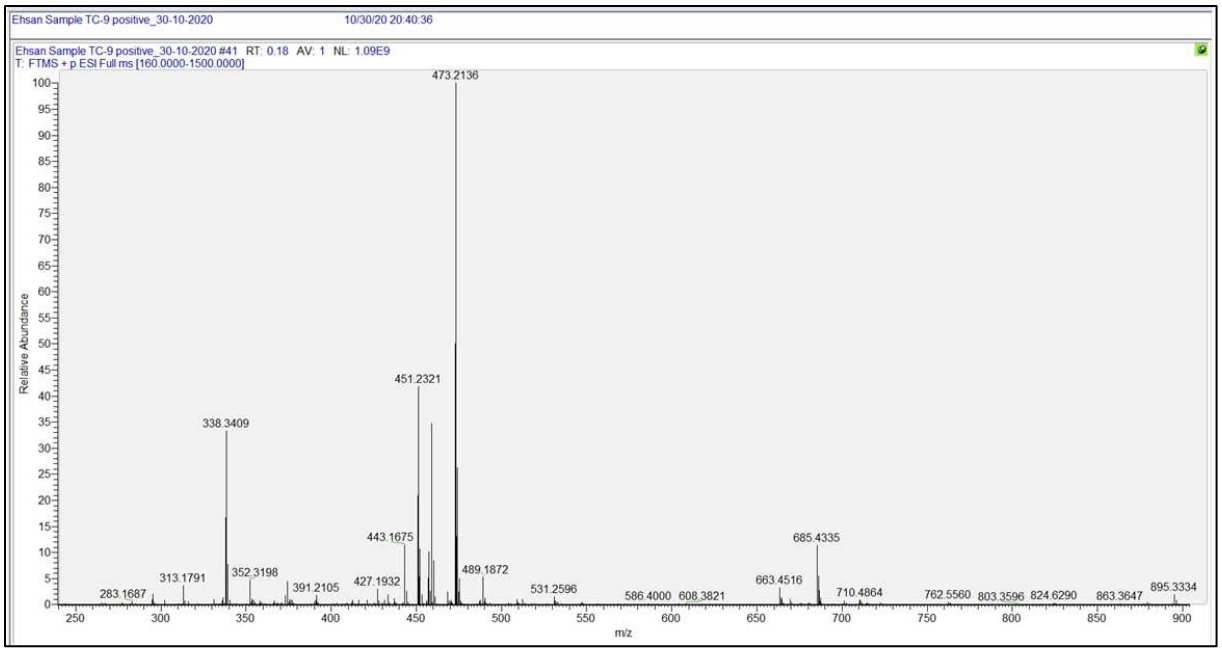

Figure S27: Positive ion HRMS of Teucretol (**7**)

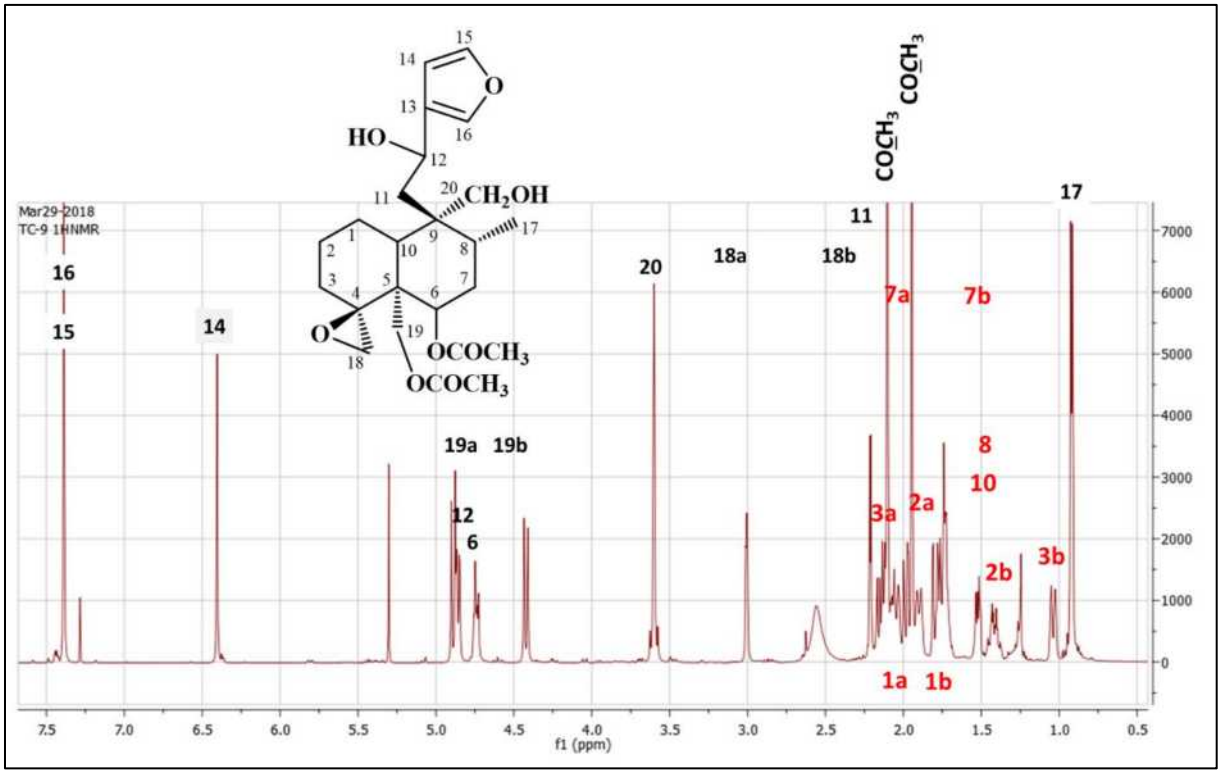

Figure S28: ^{1}H-NMR Spectrum of Teucretol (**7**) (500 MHz, CD_3OD)

© 2021 ACG Publications. All rights reserved.

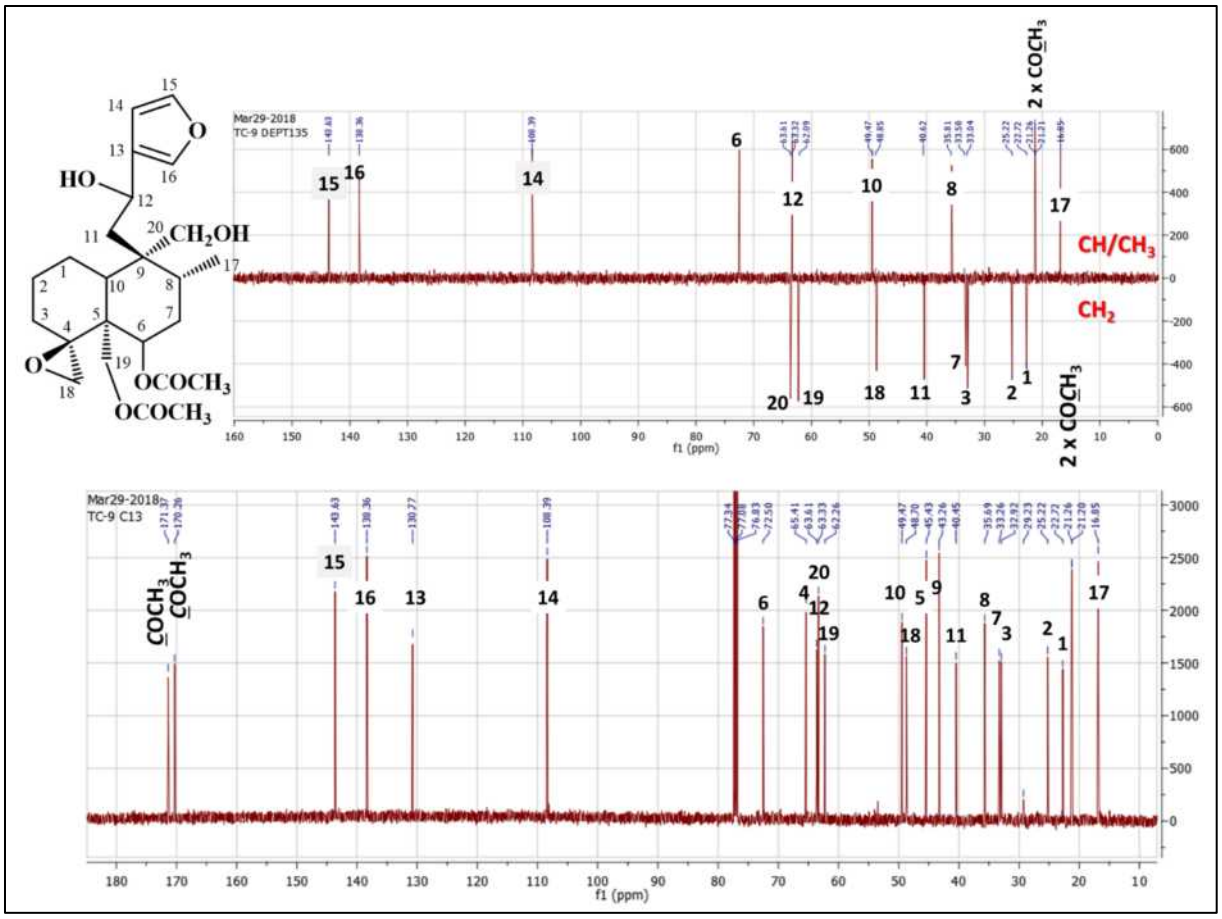

Figure S29: ^{13}C-NMR Spectrum (125 MHz, CD_3OD) and DEPT-135 of Teucretol (**7**)

© 2021 ACG Publications. All rights reserved.

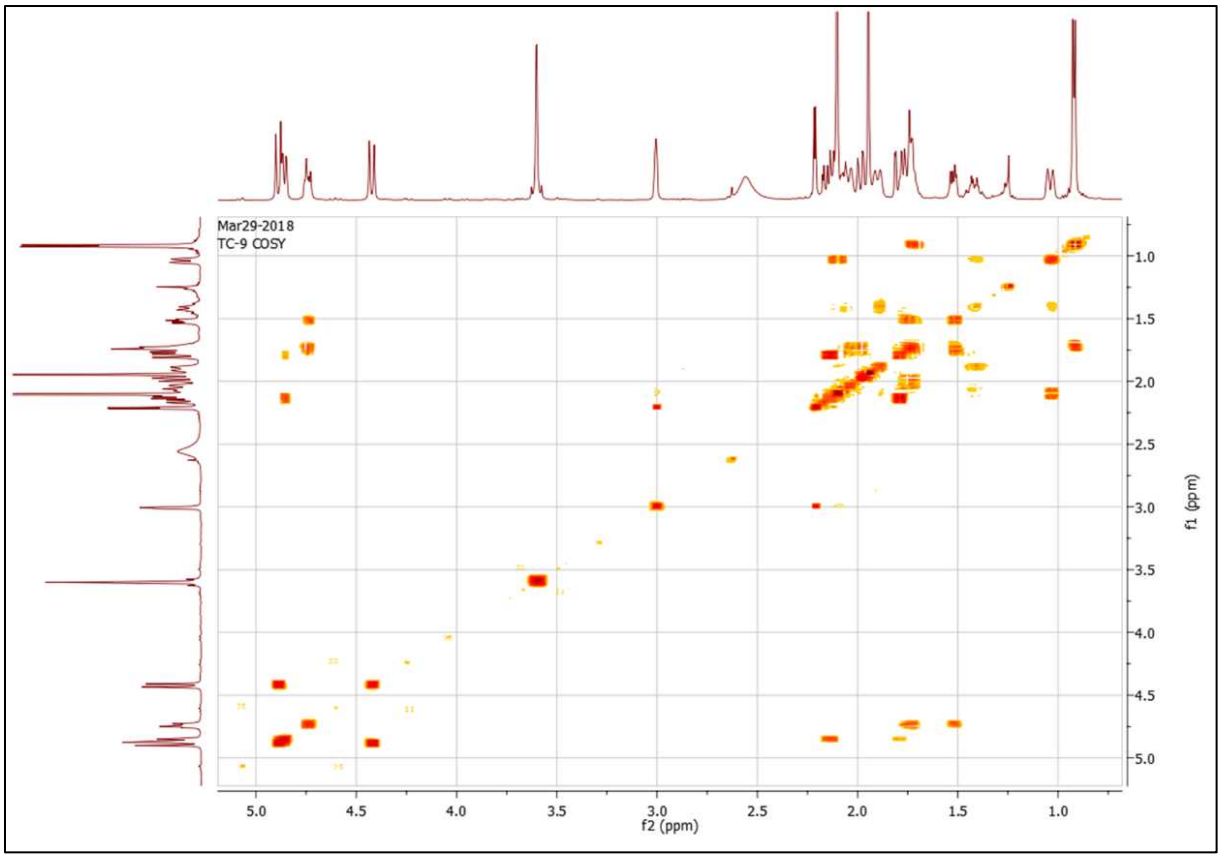

Figure S30: COSY of Teucretol (**7**)

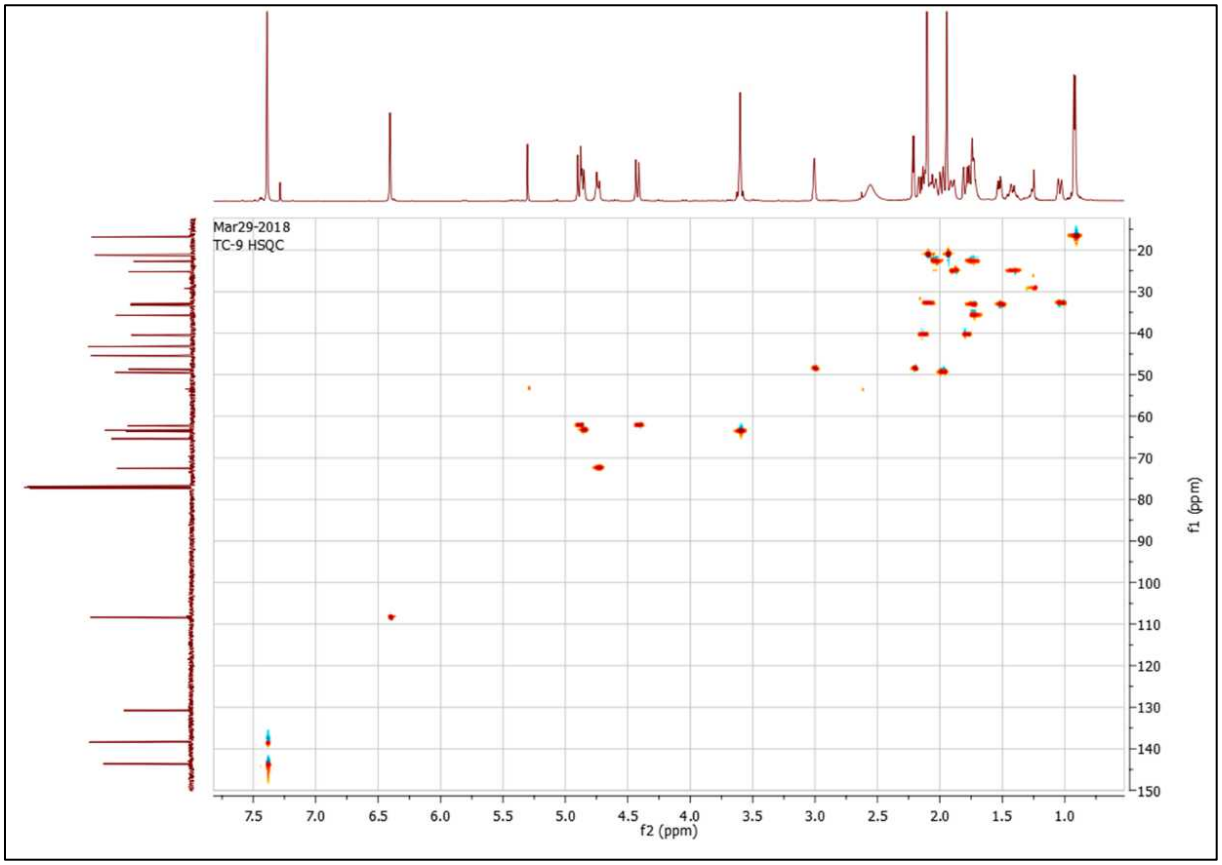

Figure S31: HSQC of Teucretol (**7**)

© 2021 ACG Publications. All rights reserved.

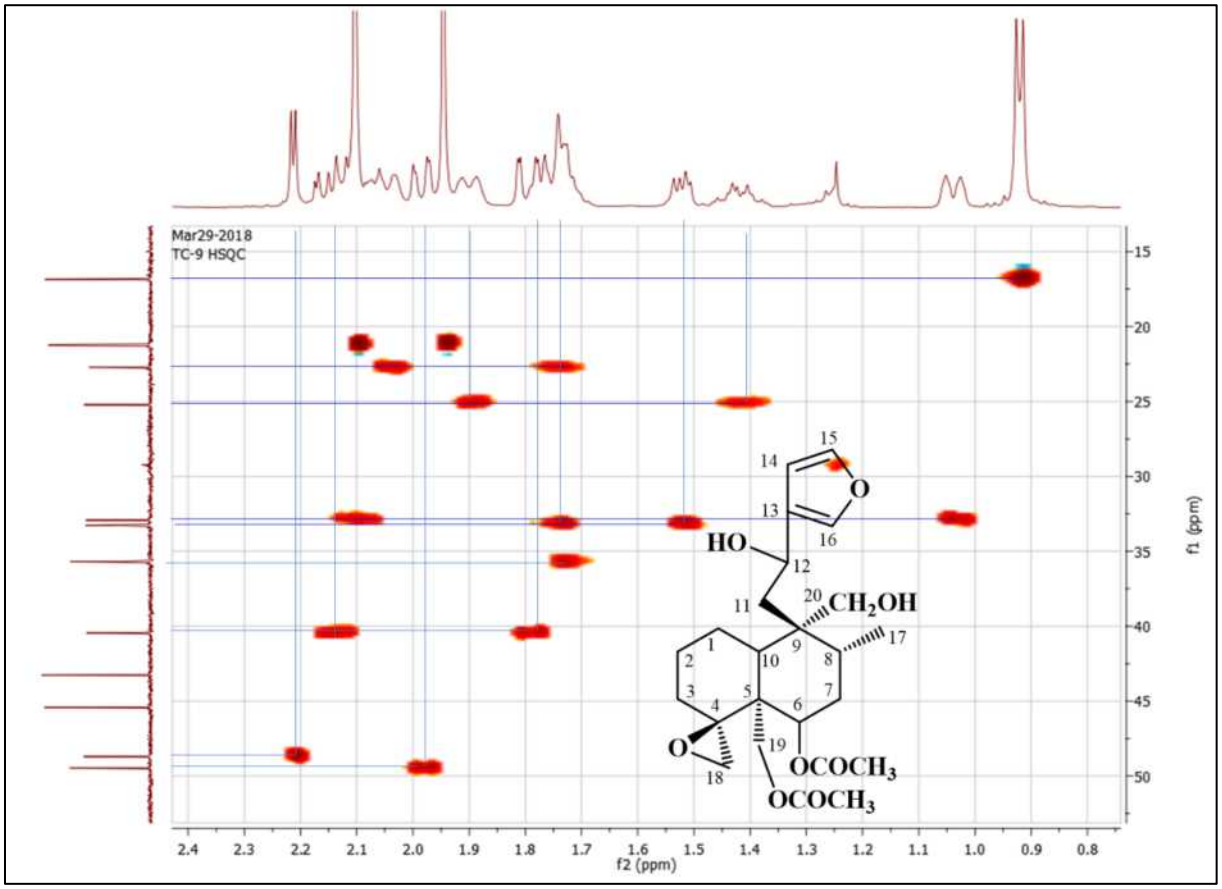

Figure S32: HSQC of Teucretol (**7**) (f1: δ 15 – 55; f2: δ 2.4 – 0.8)

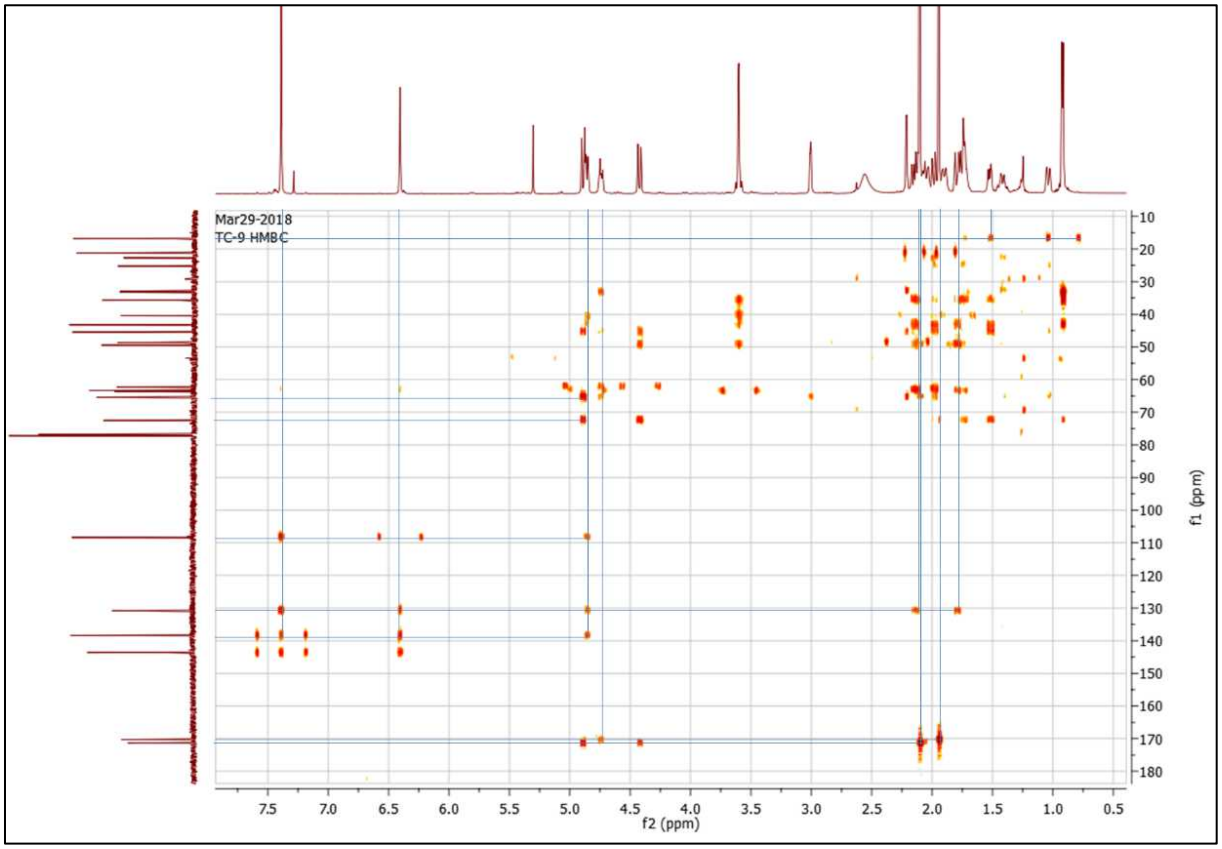

Figure S33: HMBC of Teucretol (**7**)

© 2021 ACG Publications. All rights reserved.

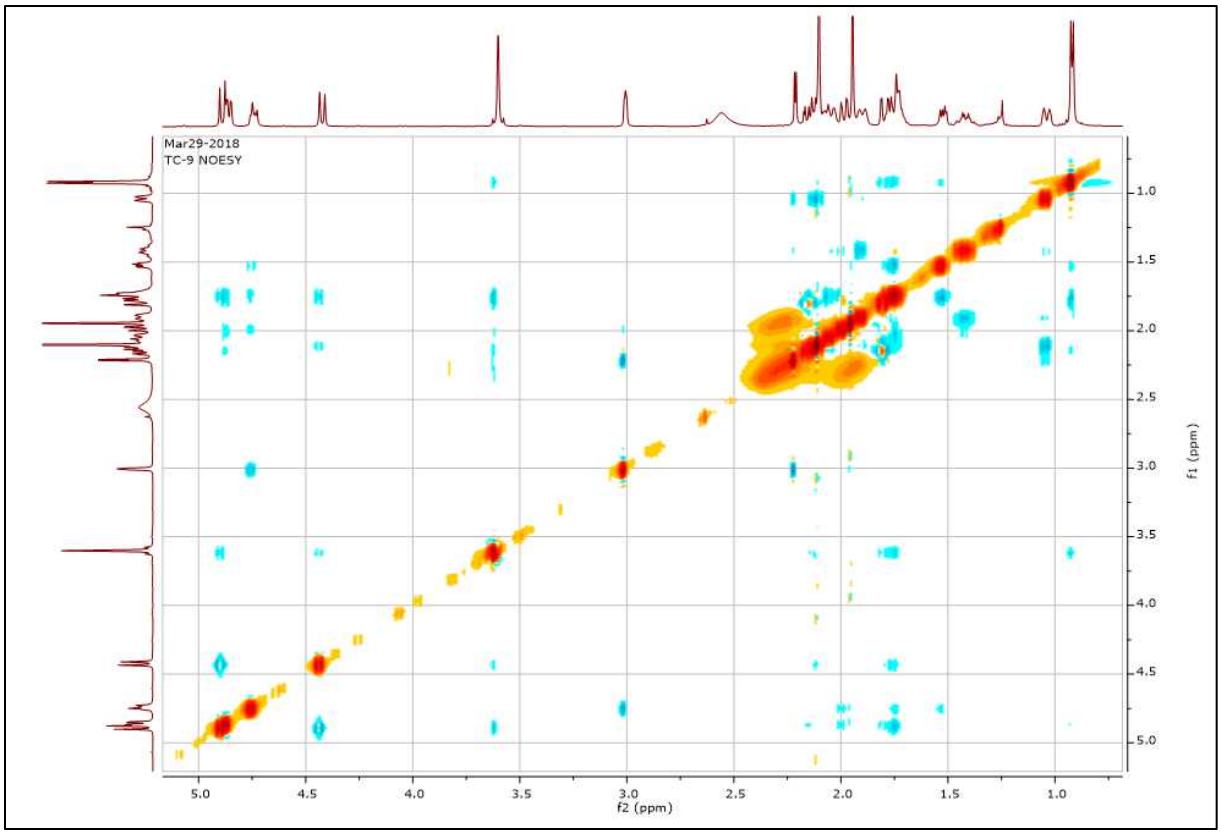

Figure S34: NOESY of Teucretol (**7**)

© 2021 ACG Publications. All rights reserved.

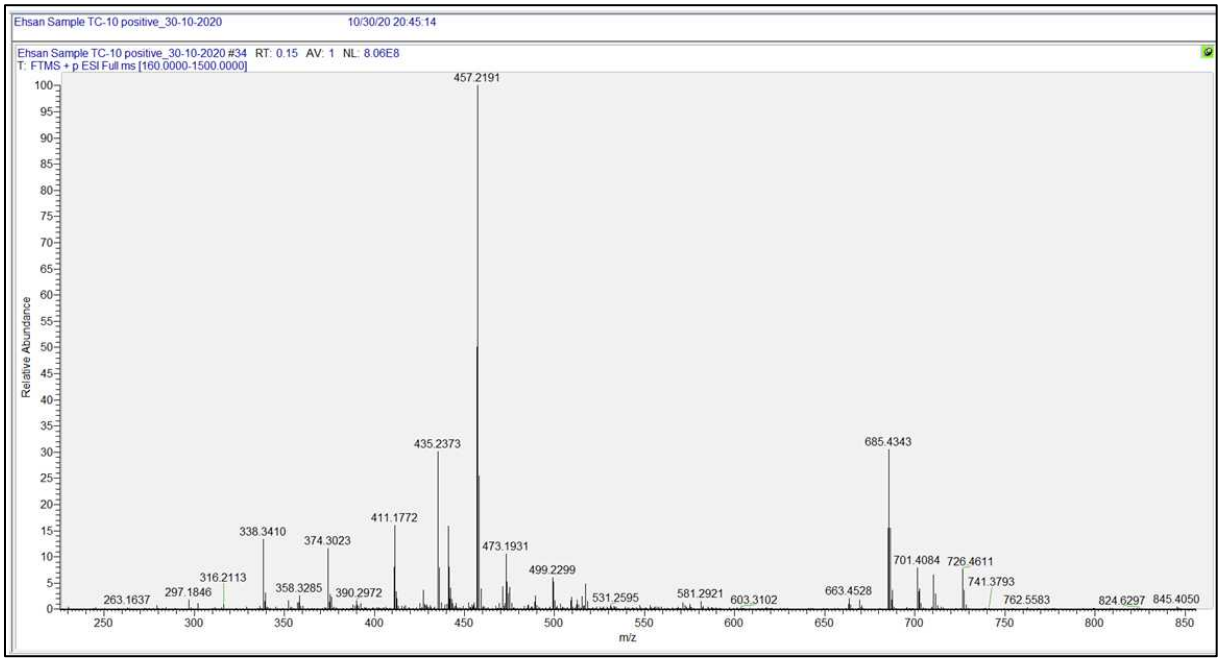

Figure S35: Positive ion HRMS of Diacetylteumassilin (**8**)

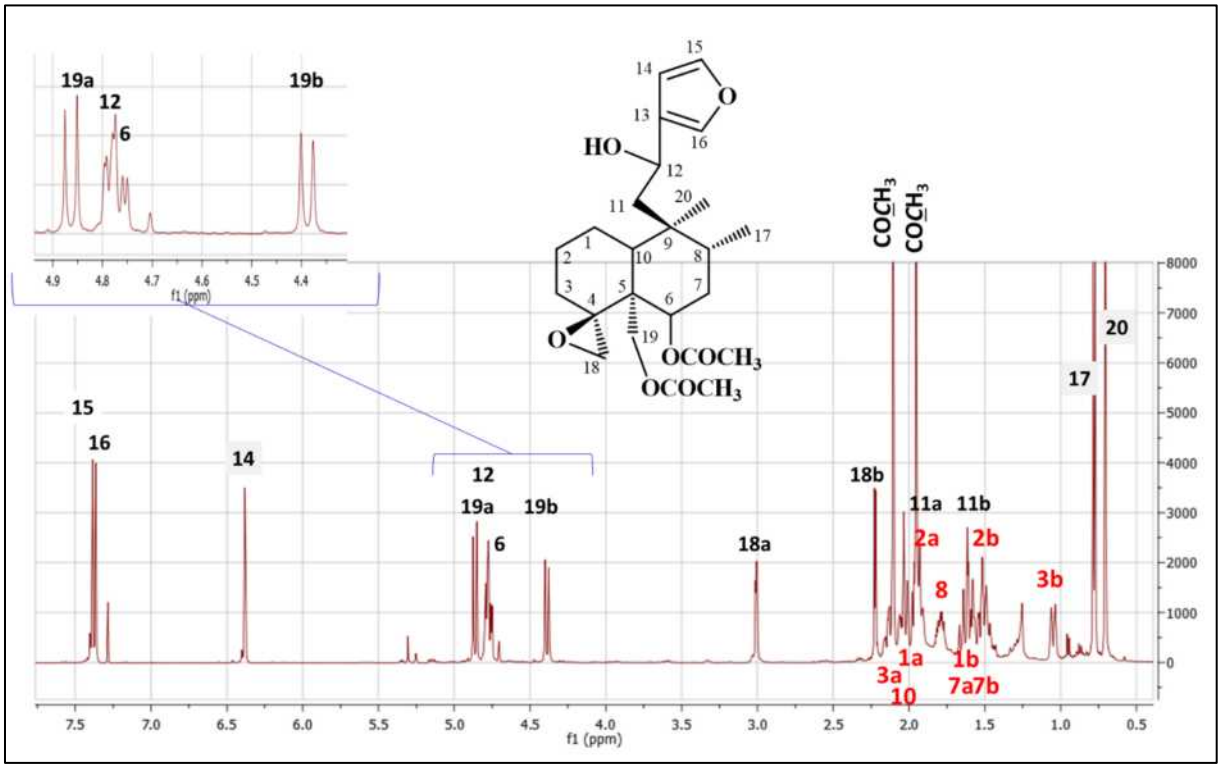

Figure S36: ^{1}H-NMR Spectrum of Diacetylteumassilin (**8**)(500 MHz, CD_3OD)

© 2021 ACG Publications. All rights reserved.

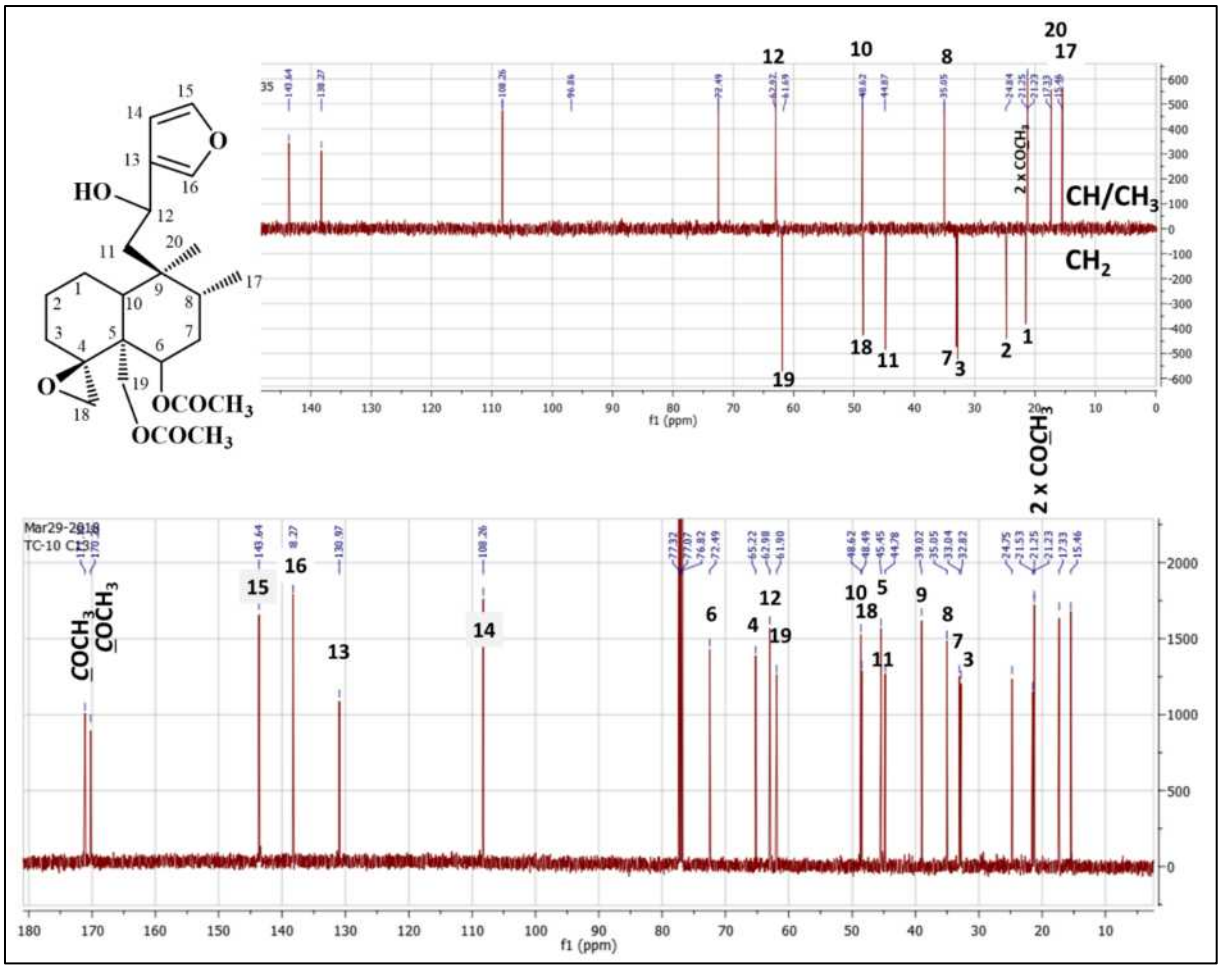

Figure S37: ^{13}C-NMR Spectrum (125 MHz, CD_3OD) and DEPT-135 of Diacetylteumassilin (**8**)

© 2021 ACG Publications. All rights reserved.

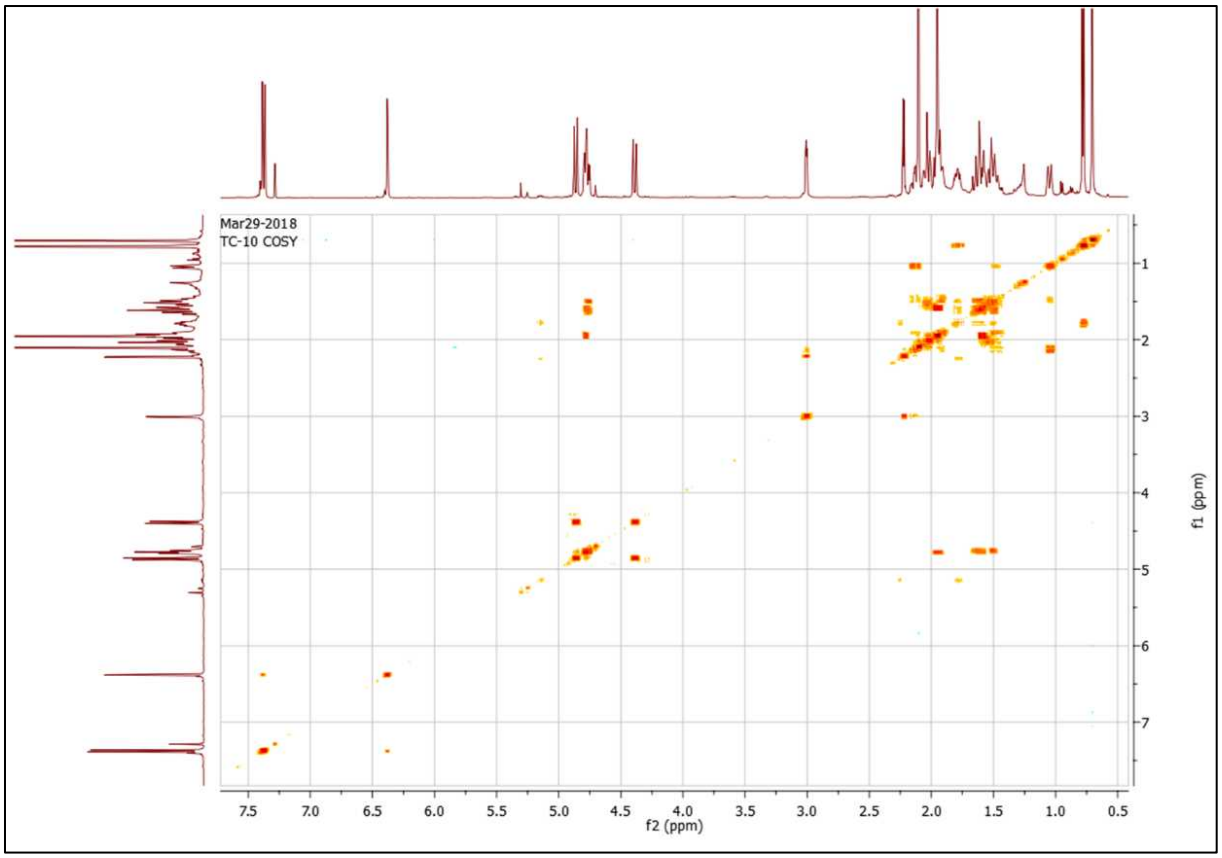

Figure S38: COSY of Diacetylteumassilin (**8**)

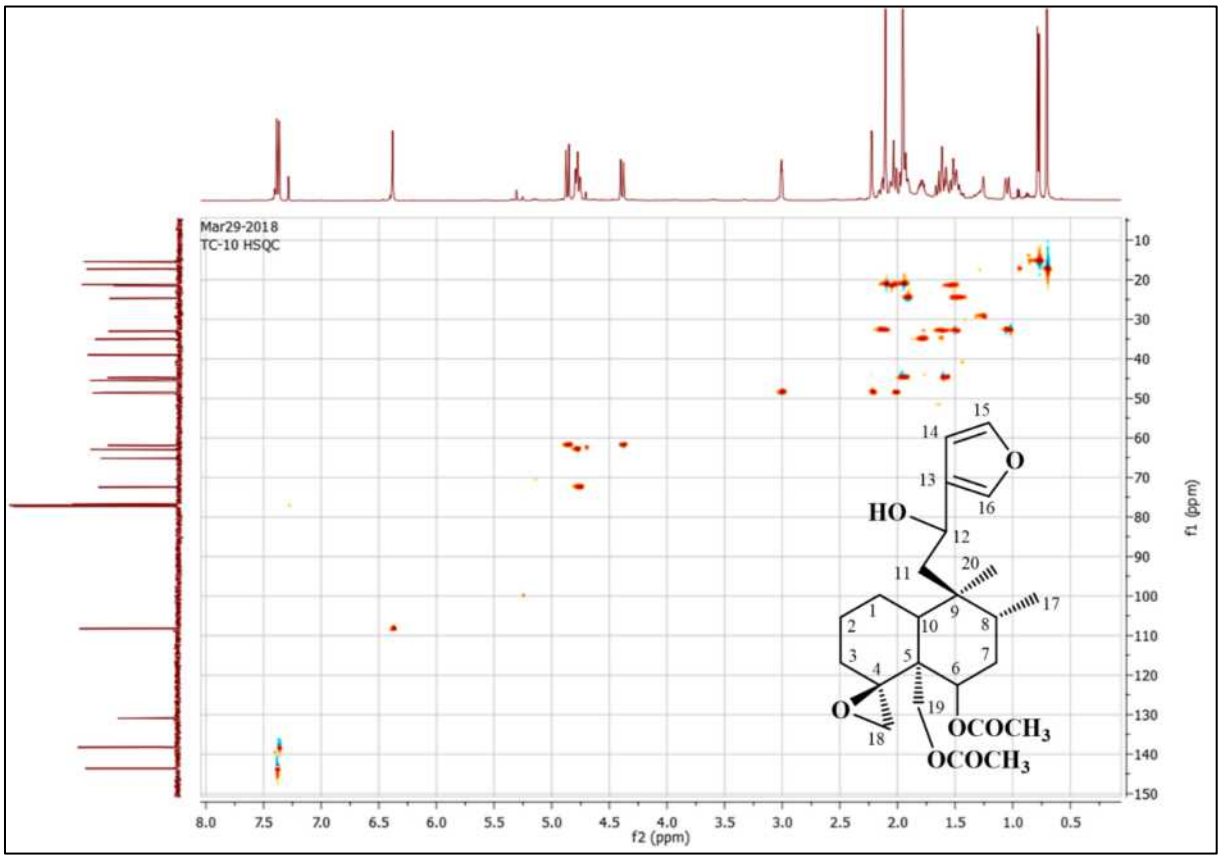

Figure S39: HSQC of Diacetylteumassilin (**8**)

© 2021 ACG Publications. All rights reserved.

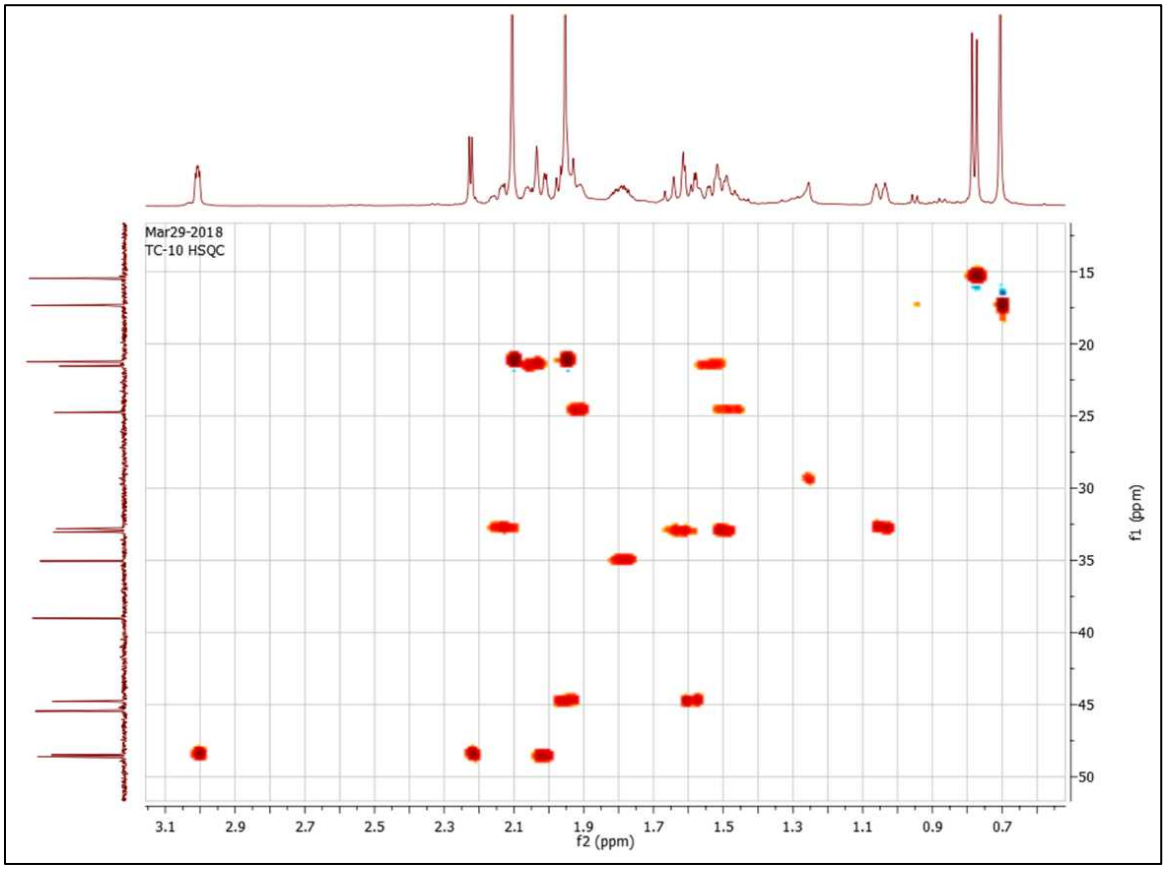

Figure S40: HSQC of Diacetylteumassilin (**8**)(f1: δ 15 – 50; f2: δ 3.1 – 0.6)

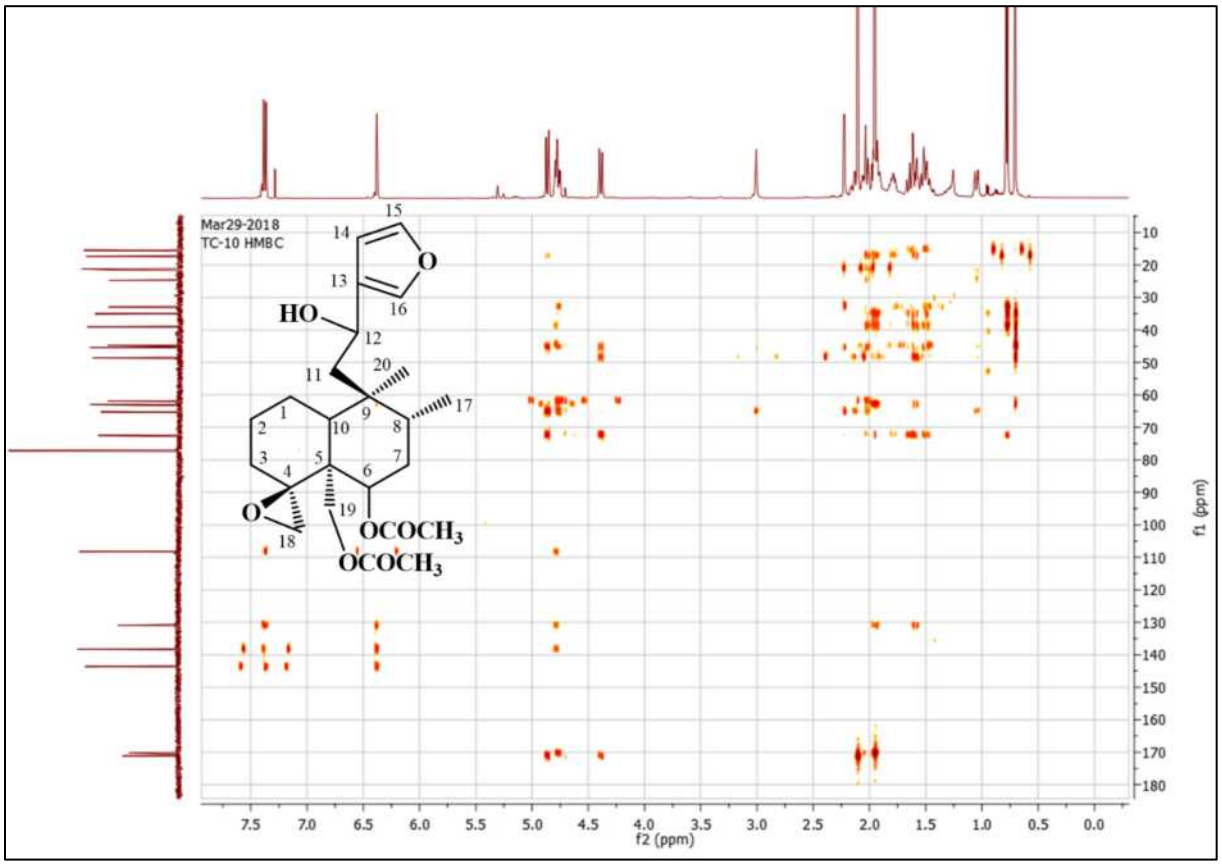

Figure S41: HMBC of Diacetylteumassilin (**8**)

© 2021 ACG Publications. All rights reserved.

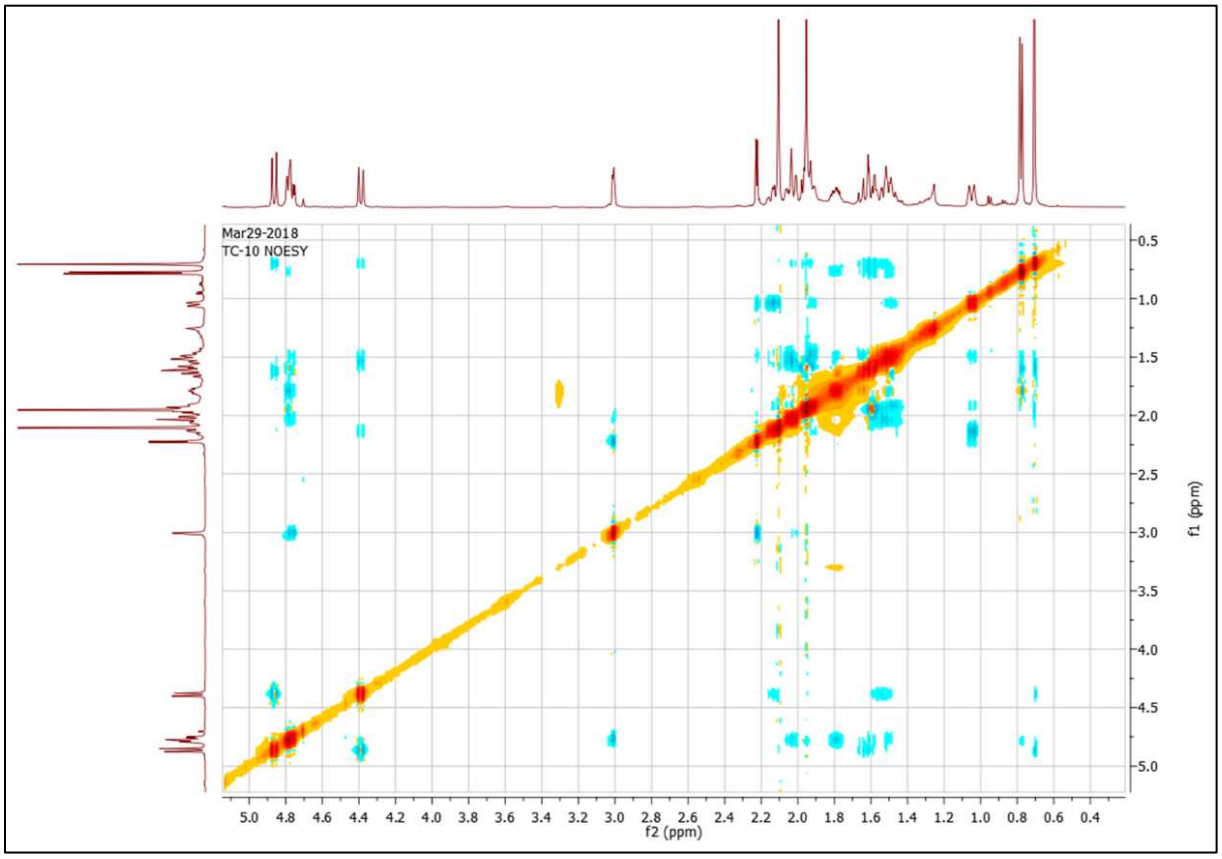

Figure S42: NOESY of Diacetylteumassilin (**8**)

© 2021 ACG Publications. All rights reserved.